CALVAL
CLS-DOS-NT-03.847
Version : 1rev0
Nomenclature : -

Ramonville, le 1er octobre 2003

Non parametric estimation of GFO sea state bias

		COMPANY	DATE	INITIALS
PREPARED BY	S. LABROUE J. DORANDEU	CLS		
QUALITY VISA	M. DESTOUESSE	CLS		
ACCEPTED BY	J. DORANDEU	CLS		
APPROVED BY	P. GASPAR	CLS		

CLS 8-10 Rue Hermès - Parc Technologique du Canal - 31526 Ramonville St-Agne - FRANCE
Téléphone 05 61 39 47 00 Télécopie 05 61 75 10 14

DISTRIBUTION LIST

COMPANY	COMPANY	COMPANY
CLS/DOS	J. DORANDEU	1
	G. DIBARBOURE	1
	P. GASPAR	1
	F. OGOR	1
	OZ. ZANIFE	1
DOC/CLS	N. ROZES	1

HISTORIQUE DES VERSIONS

VISA Gestion	VERSION	DATE	OBJET
	1REV0	01/10/2003	

A : page annulée I : page insérée M : page modifiée

GLOSSAIRE

AD	Applicable document
RD	Reference document
SSB	Sea state bias
MSS	Mean sea surface
SWH	Significant wave height
GIM	Global ionosphere maps
MWR	Micro wave Radiometer
GDR	Geophysical Data Records

Liste des tableaux et figures

List of tables :

List of figures :

DOCUMENTS APPLICABLES / DOCUMENTS DE REFERENCE

RD 1 : Dorandeu, J., G. Dibarboure, M. Ablain and Y. Faugere, 2001: Mise en place de l'acquisition et de la validation en temps réel des données GFO dans le système SSALTO/DUACS. Technical Report.

RD 2 : Gaspar, P., S. Labroue, F. Ogor, G. Lafitte, L. Marchal and M. Rafanel, 2002: Improving non parametric estimates of the sea state bias in radar altimeter measurements of sea level. JAOT, 19, 1690-1707.

RD 3 : Gaspar, P. and J.P. Florens, 1998: Estimation of the sea state bias in radar altimeter measurements of sea level: Results from a new non parametric method. J. Geophys. Res., 103, 15803-15814.

RD 4 : Gaspar, P., F. Ogor, P.-Y. Le Traon and 0.Z. Zanife, 1994: Estimating the sea state bias of the TOPEX and POSEIDON altimeters from crossover differences. J. Geophys. Res., 99, 24981-24994.

RD 5 : Labroue S. and P. Gaspar, 2001: Improvement of the sea state bias estimation. Technical Report, Contract n° 731/CNES/00/8251/00.

RD 6 : Vandemark, D., N. Tran, B. Beckley, B. Chapron and P. Gaspar 2002: Direct estimation of sea state impacts on radar altimeter sea level measurements. Geophysical Research Letters, 29, n°24, 2148.

AD 1 : GEOSAT follow-On GDR User's Handbook, NOAA, June 2002

AD 2 : SDR format, contents and algorithms

SOMMAIRE

1. INTRODUCTION

The non parametric method for estimating the sea state bias (SSB) developed by Gaspar and Florens (RD2, RD3) allows investigating the variability of the SSB as a function of the significant wave height (SWH) and an estimated wind speed (U) derived from the backscatter coefficient σ_o(Ku).

This method represents a significant improvement compared to the classical parametric methods. It better retrieves wind and wave related variations, especially for the rare sea state events, improving the SSB accuracy up to a few centimeters for some of the sea states.

It was also shown that the non parametric technique can reveal more variations in the SSB estimates since it is closer to the data than the parametric fits. It is the case for TOPEX side A and B where the non parametric estimation has detected a marked change in the SSB with the very first cycles of the side B altimeter, whereas the BM4 model has only detected a small variation between both altimeters.

The technique is now mature enough to be applied on various altimeters. It was successfully done with TOPEX, JASON 1 and ENVISAT, providing for the two latter a lookup table applied in the GDR products.

The goal of this work was thus to apply the same technique on GFO data, in order to extract a more representative signal than the BM1 model provided in the GFO GDR products.

Chapter 2 presents the data processing done to edit the measurements prior to performing the sea state bias estimation. It also highlights the main features relevant for the sea state bias field.

Chapter 3 deals with the results obtained with different SSB estimates, considering crossover data sets or direct 1Hz measurements, allowing to check the consistency of the sea state bias.

2. DATA PROCESSING

This section presents all the work done to extract an ocean data set from GFO GDR products. The first section deals with the editing performed on the data while section 2.2 sums up different investigations on the data. The section 2.3 shows the monitoring of some of the GFO parameters.

2.1. EDITING

The GDR fields are used to compute the standard sea surface height measurement with the following equation :

SSH = Orbit

- height
- dry tropospheric correction (NCEP model)
- wet tropospheric correction (radiometer)
- inverse barometer correction (NCEP model)
- ionospheric correction (GIM)
- ocean tide correction (GOT00V2)
- polar tide correction
- earth tide correction
- sea state bias correction (BM1 = 0.045*SWH)

Several parameters have also been added to these standard corrections in order to compare different models. The ECMWF dry tropospheric correction and inverse barometer correction are compared to NCEP corrections for each cycle. The GOT99 model and GOT00V2 model are also compared for the ocean tides.

The same editing processing is done for each cycle of data and it is divided into several steps:

- Checking between ascending and descending passes
- Removing land data according to altimeter quality flag (AD1)

- Editing with thresholds. The threshold values have been determined in a previous study to merge GFO data in the SSALTO/DUACS processor (RD1). The table1 gives all the details of these values.
- Editing after spline smoothing on SSH measurements in order to remove isolated erroneous points.
- Editing according to mean and standard deviation of the SLA for each pass. Passes with a mean greater than 50 cm and a standard deviation greater than 30 cm are discarded. This test allows to detect either large orbit errors or height problems.

	Threshold min	Threshold max
Orbit -Height	-110 m	+110 m
Number of height measurements	5	none
Height standard deviation	0	+0.15 m
Squared waveform attitude	-0.2 deg^2	0.13 deg^2
Dry tropospheric correction	-2.5 m	-1.9 m
Inverse barometer correction	-2 m	+2 m
Wet tropospheric correction	-0.5 m	-0.001 m
Ionospheric correction	-0.4 m	+ 0.04 m
SWH	0 m	12 m
Sea sate bias BM1	-0.5 cm	0 m
Sigma0	7 dB	30 dB
Ocean tide	-5 m	+5 m
Earth tide	-1 m	+1 m
Polar tide	-15 m	+15 m
SSH -MSS CLS 01	-10 m	+10 m

Table 1 - Threshold values for the editing

For each cycle, a synthesis report is generated with the results of the editing, various statistics on the cycle crossover data set and the different maps and histograms for the altimeter parameters and the geophysical corrections. Particular attention is paid to the maps of the edited measurements depending on the considered parameter. An example of such a report for the cycle 38 is given in annex.

2.2. PARTICULAR INVESTIGATIONS

2.2.1. Recurrent edited segments

For each processed cycle, the map of the edited measurements exhibits several recurrent segments of ocean measurements. There are always located in the same region for each cycle. Two parameters are rejected for these data : the squared attitude and the wet tropospheric correction. An analysis on one cycle has shown that these segments have all the values of the squared attitude set to a default value and the values for the wet tropospheric correction set to zero. Figure 1 shows the map obtained for the cycle 91. After investigation, NOAA has found out it was a problem of telemetry which happened at the end of each SDR products.

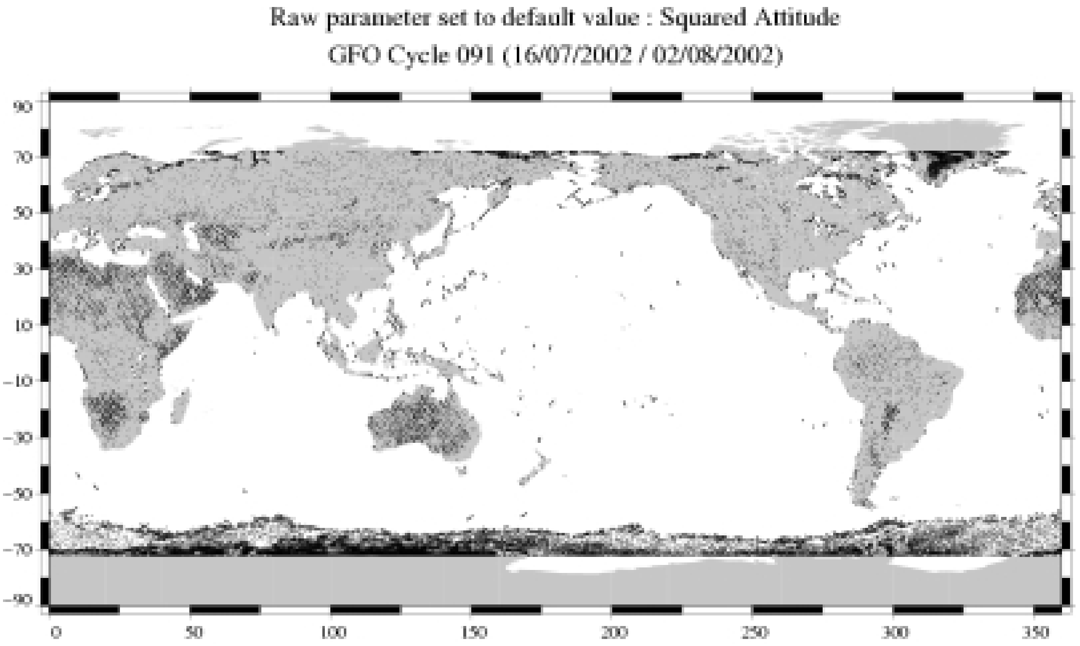
Raw parameter set to default value : Squared Attitude
GFO Cycle 091 (16/07/2002 / 02/08/2002)

Figure 1 - Map of the measurements with the squared attitude set to default value

2.2.2. Squared attitude

For most of the processed cycles, the histogram of the squared attitude exhibits two populations and it is far from being a gaussian law as it is expected. This trend varies also with time. Actually, it comes from the way of computing the squared attitude.

$$\text{Attitude\_Squared} = b1^2 *(\text{ Fitted\_VATT} - b0) \text{ with } b0=1.11 \text{ and } b1=0.8747 \qquad (1)$$

Fitted_VATT is computed at 1Hz by a linear fit of the average VATT on a sliding 1 minute data span.

Average VATT is the mean of the 10 Hz values of average VATT. It is the value the closest to the waveform since it is a simple mean of the 10 Hz values. The histogram of the average VATT is gaussian and it is the way of smoothing when computing Fitted VATT which makes the two populations appear in the histograms of fitted VATT and squared attitude. One can refer to the results for the cycle 38 presented in appendix A.

More surprisingly, the maps of Average VATT show a signature between ascending and descending passes and north and south hemisphere. The signature is even more marked for Fitted VATT and it varies with time, different patterns appearing depending on the cycle considered. It seems that it is mainly the maps of descending passes which exhibit a clear transition between both hemispheres.

2.2.3. Height correction

In the document AD1, the height correction is defined as the sum of four terms :

Height_Correction = Attitude_Wave_Height_Bias
- Height_Calibration_Bias
+ Altitude_Bias_Center_of_Gravity
- Altitude_Bias_Initial
- FM_Crosstalk

where Height_Calibration_Bias, Altitude_Bias_Center_of_Gravity and Altitude_Bias_Initial are constant for all the cycles.

FM_Crosstalk is the Doppler correction computed from the height rate

Attitude_Wave_Height_Bias is the correction depending on SWH and Fitted VATT

We are interested in this correction since it depends on SWH and it may explain some features of GFO sea state bias.

Unfortunately, the Doppler correction is not available in the GDR products to compute directly the height correction depending on SWH and attitude.

We recompute the height rate with the orbit given in the GDR products and from this calculation, we derive the Doppler correction with the following equation given in AD2:

$$\text{Doppler\_Effect} = (46.38096/107.4) * \text{Height\_rate} = 0.4318 * \text{Height\_rate} \qquad (2)$$

Then, we can deduce the correction depending on SWH and attitude by the following combination :

$$\text{Attitude\_Wave\_Height\_Bias} = \text{Height\_Correction} + \text{Doppler\_Effect} + \text{constant} \qquad (3)$$

This is done routinely for each cycle and a scatter plot with SWH is given to quantify roughly the dependence of this correction with SWH. On all cycles, the height correction presents a dependence of around 1.5% of SWH, as a first approximation. The scatter plot clearly shows the effect of the gate index on the correction.

The same scatter plot is made with the fitted VATT parameter instead of SWH. The dependence with the attitude is less marked than the one with SWH, but it also shows the influence of SWH with the different scatters of points corresponding to the different class of SWH. One can notice that the influence of the attitude is greater for high SWH.

2.3. PARAMETERS MONITORING

We processed GFO data from cycle 37 to 91, from January, 2000 till July, 2002. A monitoring of all the parameters is done cycle by cycle and day by day to detect potential trends or unexpected signals.

The following figures present some results for the main altimeter parameters.

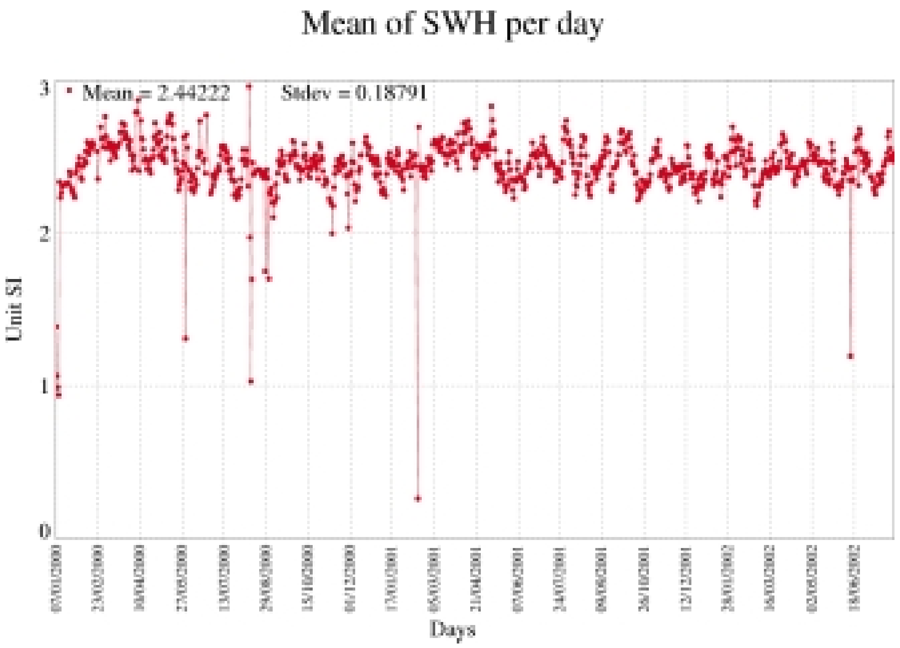

Figure 2 - Mean of SWH per day, after editing

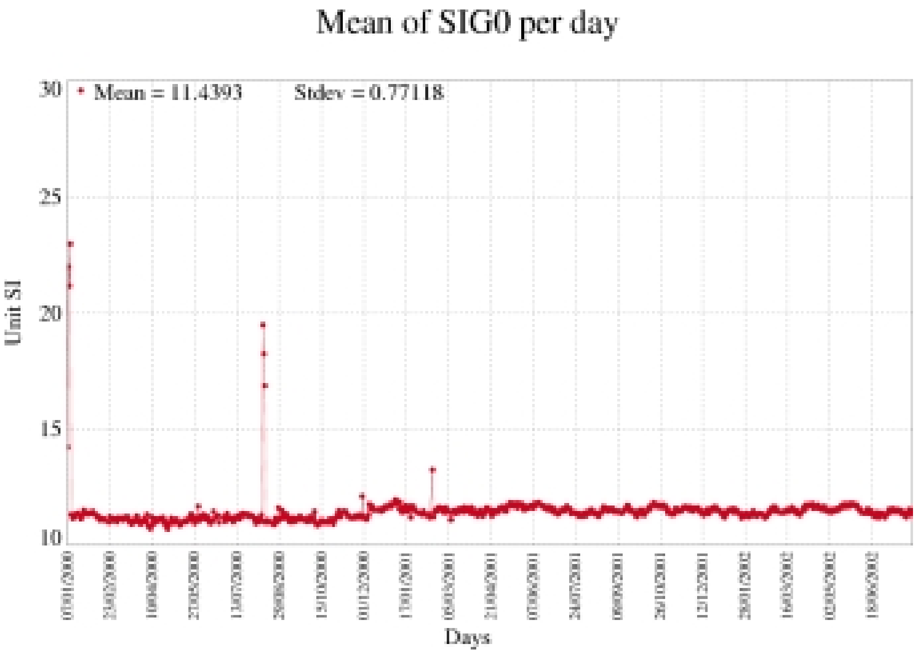

Figure 3 - Mean of Sigma0 per day, after editing

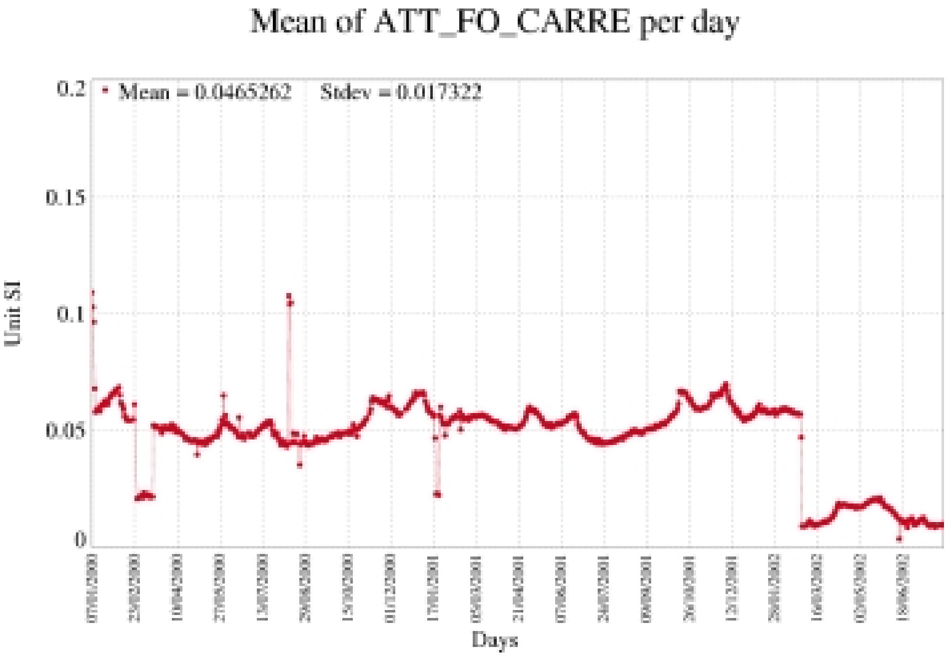

Figure 4 - Mean of squared attitude per day, after editing

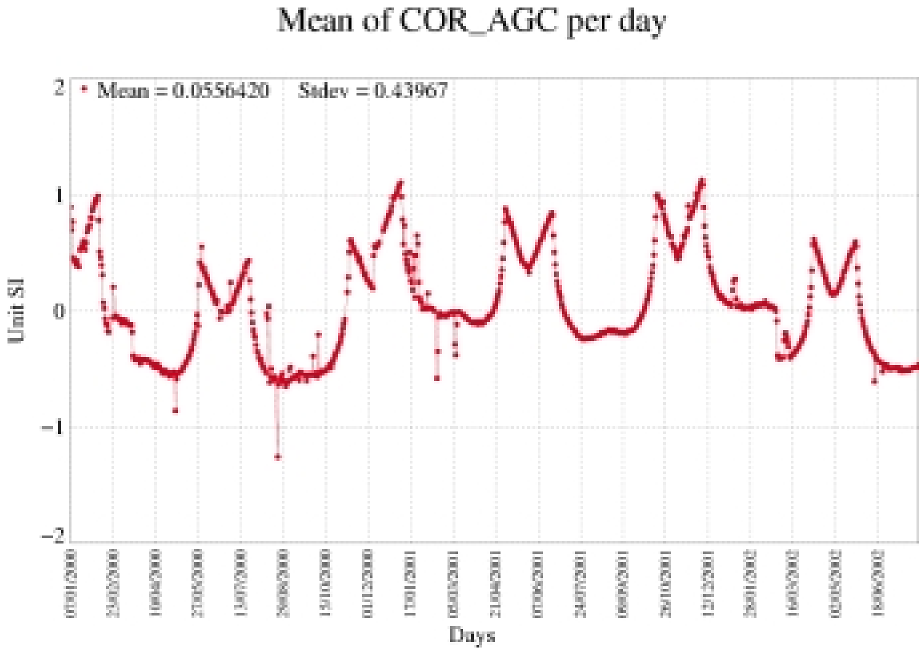

Figure 5 - Mean of AGC correction per day, after editing

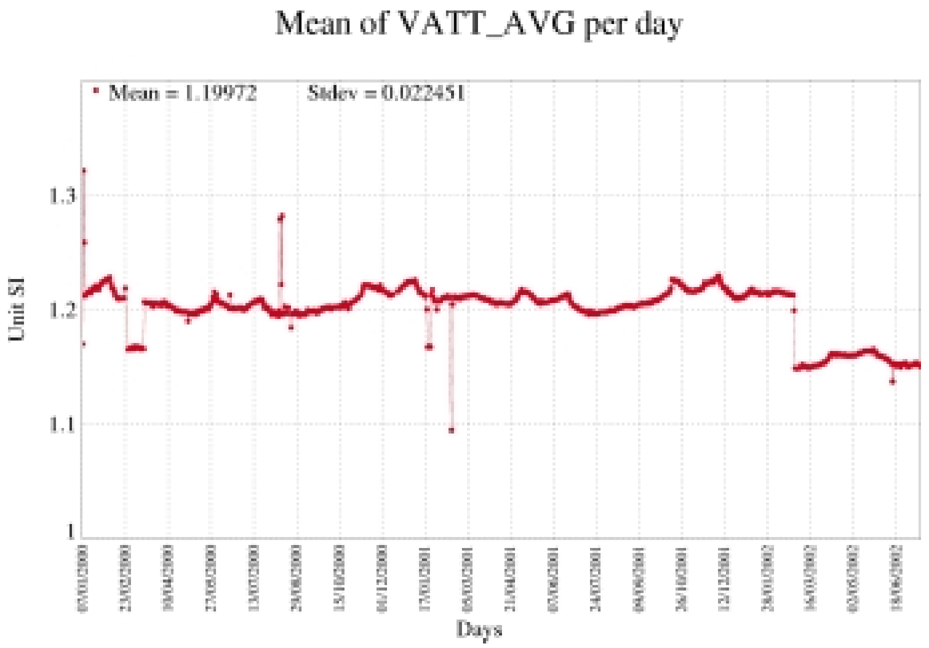

Figure 6 - Mean of average VATT per day, after editing

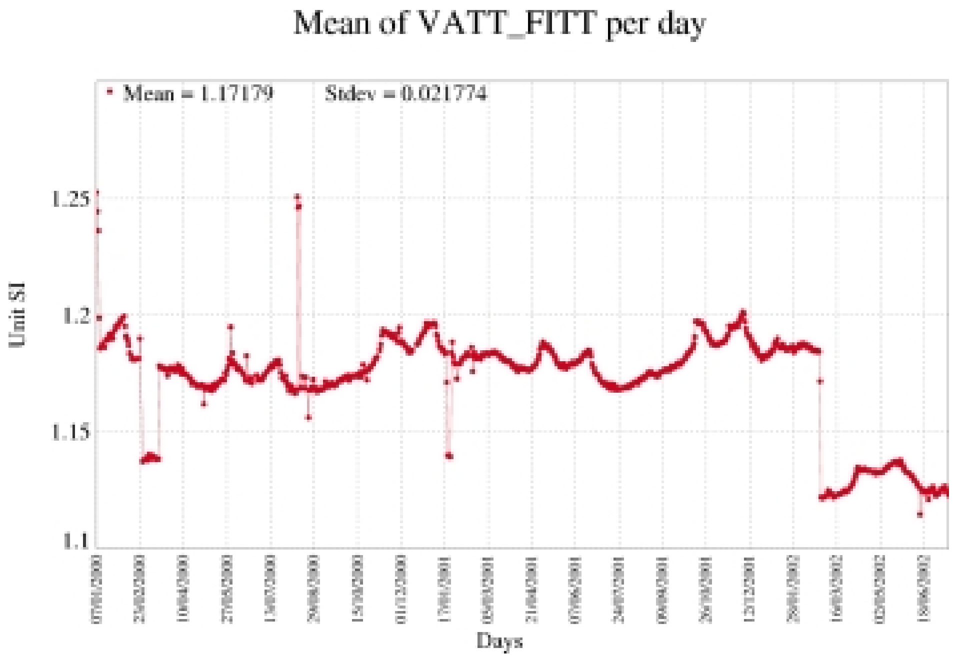

Figure 7 - Mean of fitted VATT per day, after editing

3. SEA STATE BIAS ESTIMATION

This section presents the results obtained with two different approaches for the estimation of the sea state bias : the classical one using crossover differences of SSH and the direct method using sea height residuals (DR 6).

3.1. CROSSOVER ESTIMATION

3.1.1. Crossover data sets

The SWH histogram on figure 8 exhibits a strong quantification which is also present on the distribution density in the (U,SWH) plane (Figure 9). There is also a marked discontinuity at SWH=3m on both figures 8 and 9. One can notice a peak of data for U=1m/s which probably comes from the MCW wind speed algorithm.

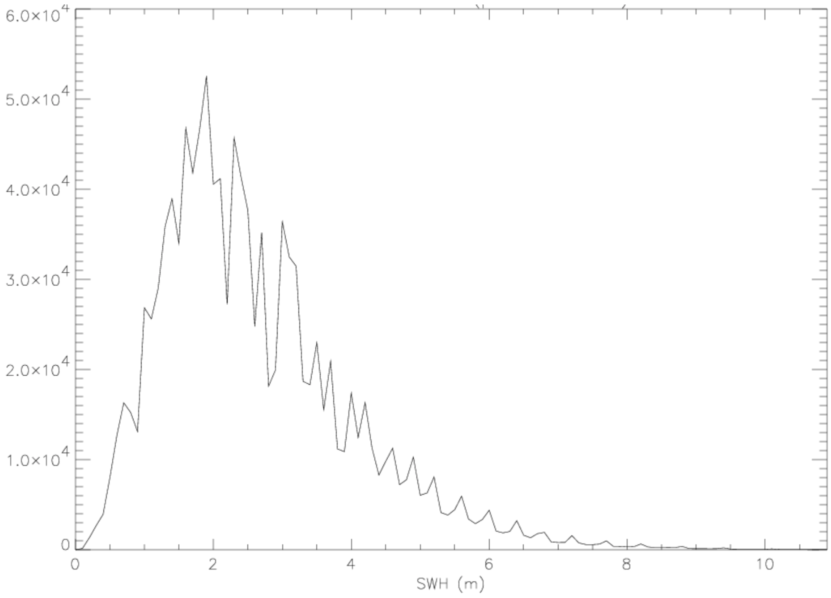

Figure 8 - SWH histogram for all the 10 days crossovers

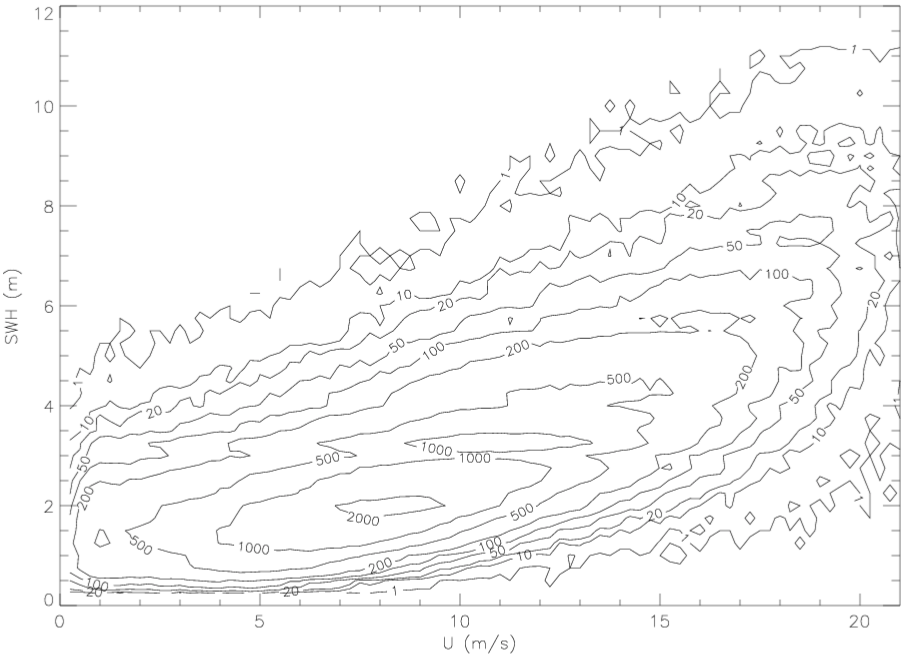

Figure 9 - (U,SWH) distribution for all the 10 days crossovers

The crossover points within a cycle give differences of SSH with a temporal variation between 0 and 17 days which can induce too large oceanic variation. To be closer to TOPEX or JASON configuration, crossover data sets are computed using 10 day data sets without taking into account the GFO cycles. Indeed, selecting SSH differences with time differences less than 10 days within the 17 days crossover data set, would induce a larger mean time tag.

Working with the data from January 2000 till July 2002 makes a total of 93 data sets of 10 days crossover differences. They are divided into 3 sets of nearly 30 cycles each to cover nearly one year of data.

The sea state bias is estimated for each cycle and then an average of all the estimates is done for several cycles. The individual estimation is done with larger bandwidths than for TOPEX. The initial bandwidths are of 1.5 m for SWH and 3 m/s for the wind speed. A factor taking into account the data distribution is also applied, depending on the grid point considered.

Figures 10, 11 and 12 give the estimates obtained for the three periods. The three estimations exhibit the same variations related to the waves and wind speed. The variations are very linear for SWH less than 2m and there is a change in the wind speed derivative around 12 m/s as it is observed for all the altimeters. The magnitude of the SSB is of the same order for the two first data sets with a value between -19 cm and -20 cm at the distribution centre (SWH=2m and U=8m/s) and a value between -43 cm and -45 cm for high waves of 6m. The third estimate gives lower values but there are still larger than the expected -10 cm value at the centre of the distribution, more in agreement with the BM1 model of the GDR products.

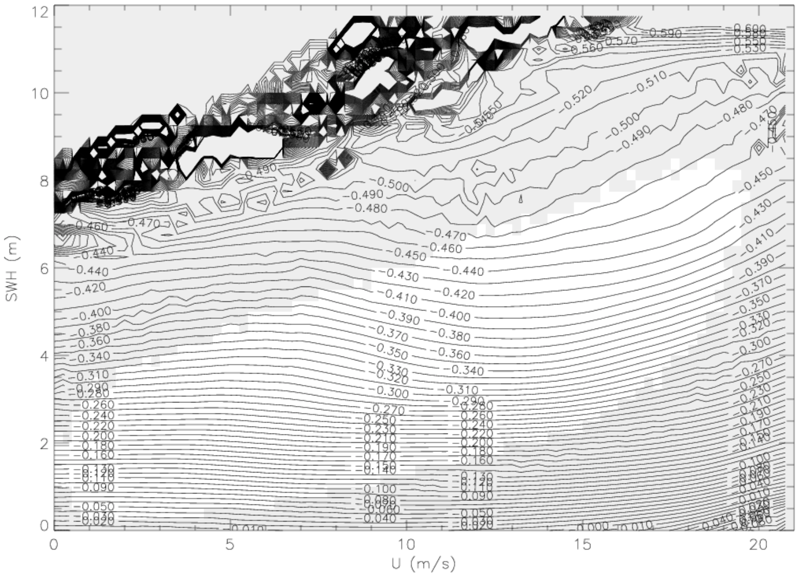

Figure 10 - SSB estimated with 10 days crossover of the first period CROSS1

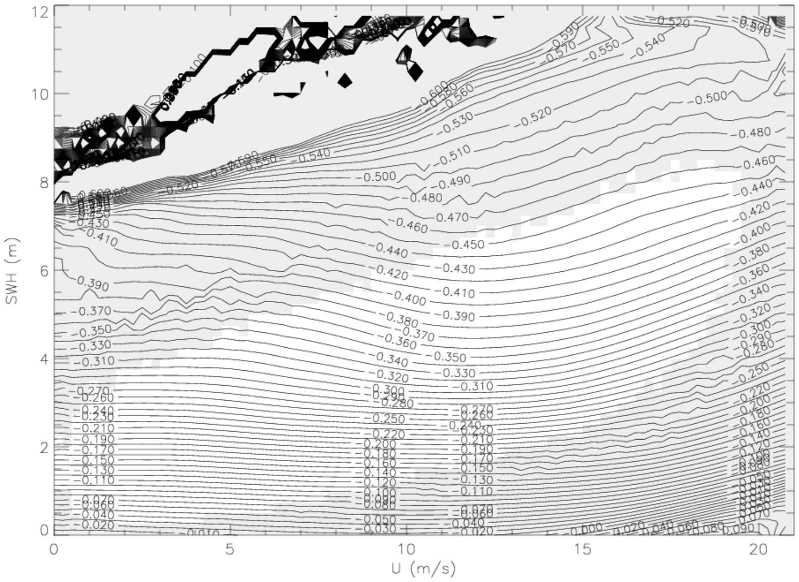

Figure 11 - SSB estimated with 10 days crossover of the second period CROSS2

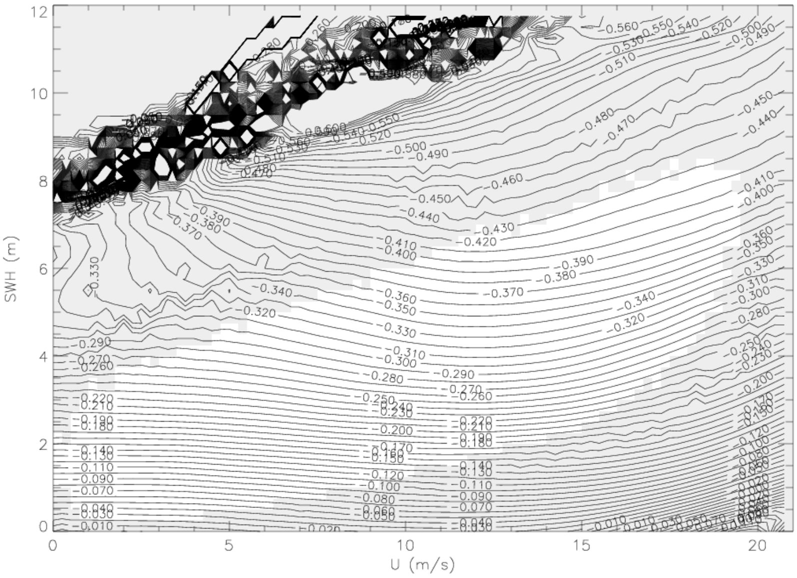

Figure 12 - SSB estimated with 10 days crossover of the third period CROSS3

The analysis of the individual estimates shows larger variations of the SWH gradient from one data set to another. To confirm this visual analysis, the value of the estimation obtained for the grid point (SWH=2m, U=3m/s) is monitored for all the individual estimations. Figure 13 shows temporal variations too large (10cm of magnitude) to be correlated with the seasonal signal of the waves and wind speed.

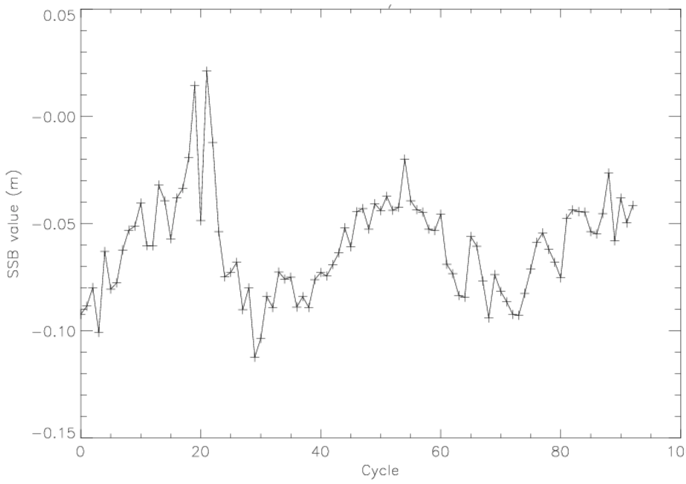

Figure 13 - Evolution of the SSB estimated value at (SWH=2m,U=3m/s)

We should recall that, in the non parametric processing, all the estimates are constrained at (SWH=2.7m, U=8m/s) to a fixed SSB value. For GFO, it was set to 5% of SWH ie around -13.5cm and thus, the SSB value at (SWH=2m, U=3m/s) should be of the same magnitude, around -10 cm. Such a constraint helps to fix the magnitude of the SSB but has no impact on the shape of the estimates. All the estimates are determined with the same value fixed in the distribution centre, letting the estimate fit the data in the other parts of the (U,SWH) domain. After averaging the individual estimates, the final solution is shifted to fulfill the condition SSB(0,0)=0m.

A comparison is also made with the direct method to check if the same SSB variations are retrieved considering a different data set. For the 3 periods, the SLA data are simply binned in (U,SWH) boxes without smoothing with the non parametric estimator, in order to quickly check the consistency with the crossover estimates. The results with the SLA data are consistent between the three periods. Figure 14 shows the third data period and even if the data are not smoothed, one can clearly see that the SWH gradient between 0 and 2m is much smoother than the one observed on the crossover estimation, with a value closer to 11 cm instead of 15 cm. The magnitude of figure 14 is closer to the 4.5% of the BM1 model and we should retrieve it through crossover and SLA data sets. This implies that there is something in the crossover data that explains the unexpected results for the SSB.

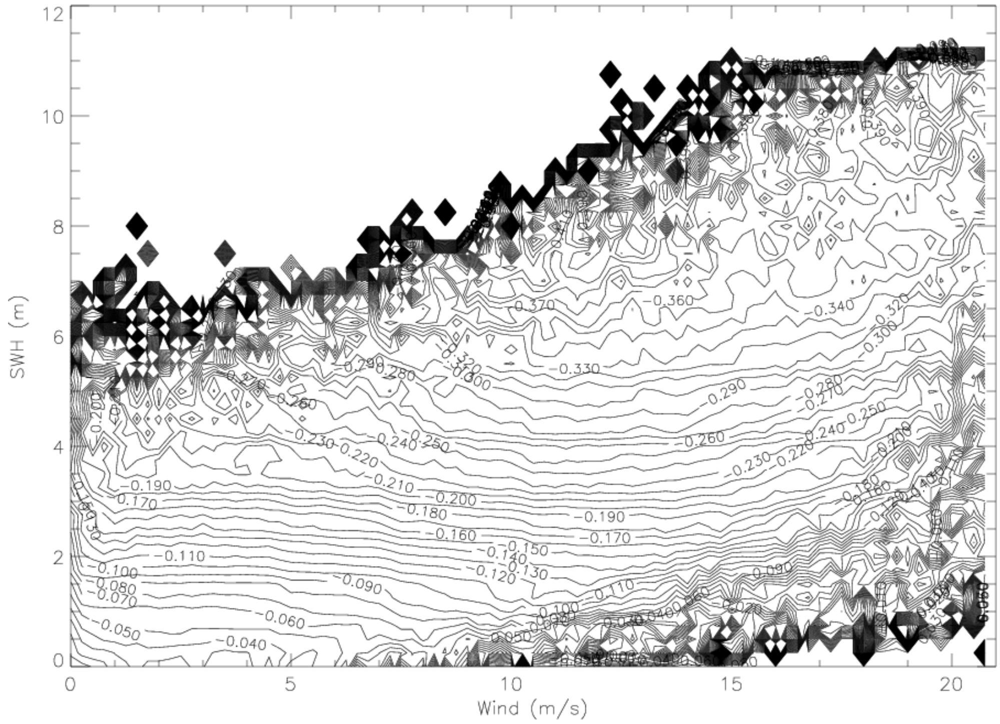

Figure 14 - SLA binned into (U,SWH) boxes, period from 28/09/2001 till 15/07/2002

Figure 15 shows the mean of the SSH crossover differences used for the SSB for each data set. The general shape is well correlated with the SSB variations observed on figure 13.

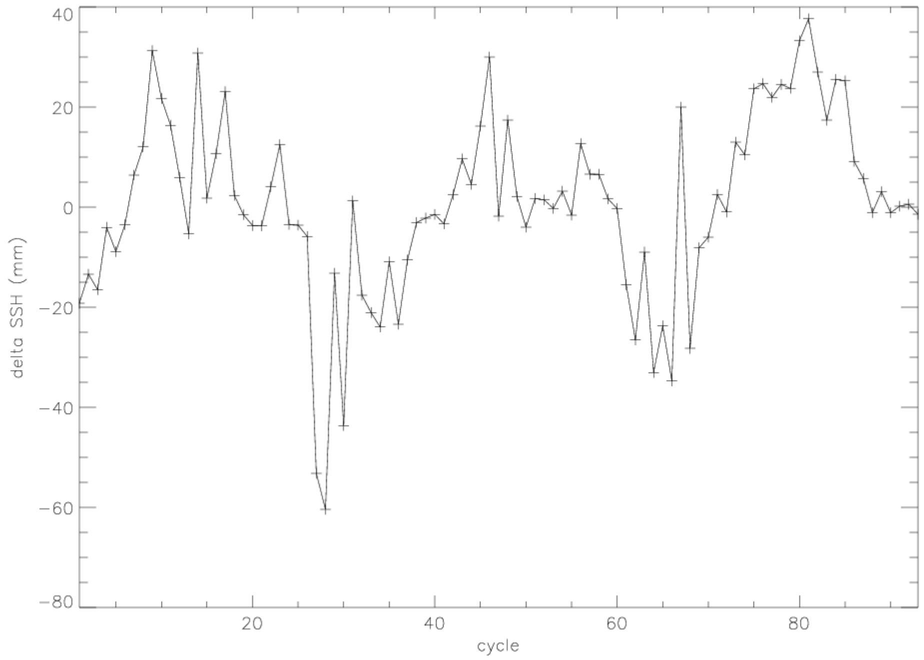

Figure 15 - Mean of SSH differences used for the SSB estimation at crossovers

The SSB temporal variations seem to come from one component of the SSH measurement. The geophysical corrections (tropospheric correction, ionospheric correction and tides correction) are unlikely to induce such a large signature with SWH. It is more probably the height measurement or the height correction, since it depends on SWH for one part.

Figure 16 exhibits the same analysis than figure 15 for the crossover differences of the height correction. Again, it shows the same signature and the peaks of the height correction match the ones observed on the SSH differences, with opposite signs.

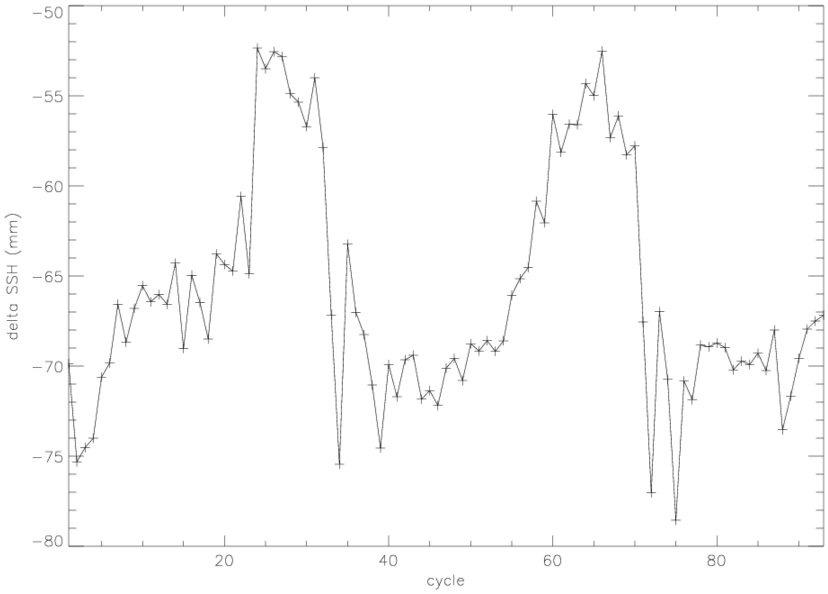

Figure 16 - Mean of differences of height correction at crossovers

3.1.2. Analysis of height correction and height rate in (U,SWH) plane

In this section, we look more in details at the height correction and how the crossover differences can make such variations in the SSB estimation.

The (U,SWH) related variations of the height correction are analyzed at crossover differences and with the along-track measurements to try to explain the difference seen in the SSB estimates. We focused on the year 2000 for the along-track data and we use all the 10 day data sets for the crossovers.

Figure 17 exhibits the mean of the height correction crossover difference binned into (U,SWH) boxes and figure 18 the height correction binned into (U,SWH) boxes. Actually, the SLA data present a nearly constant correction for SWH<1.5m whereas the crossover differences exhibit a stronger SWH gradient for SWH<2m. It confirms that this correction has an opposite effect on SWH depending on whether crossover differences are considered or not. The large magnitude observed for the height correction in figure 18 is due to the sum of the three constant biases applied for all cycles.

Figure 19 and 20 also show the height correction but distinguishing between ascending and descending tracks for along-track data, on the same period. They present a significant difference for SWH<3m. The ascending tracks have a regular SWH gradient of 6 cm between 0.5m and 2m of waves. The descending tracks show a peak for SWH=2m and U<5m/s and thus a less regular gradient.

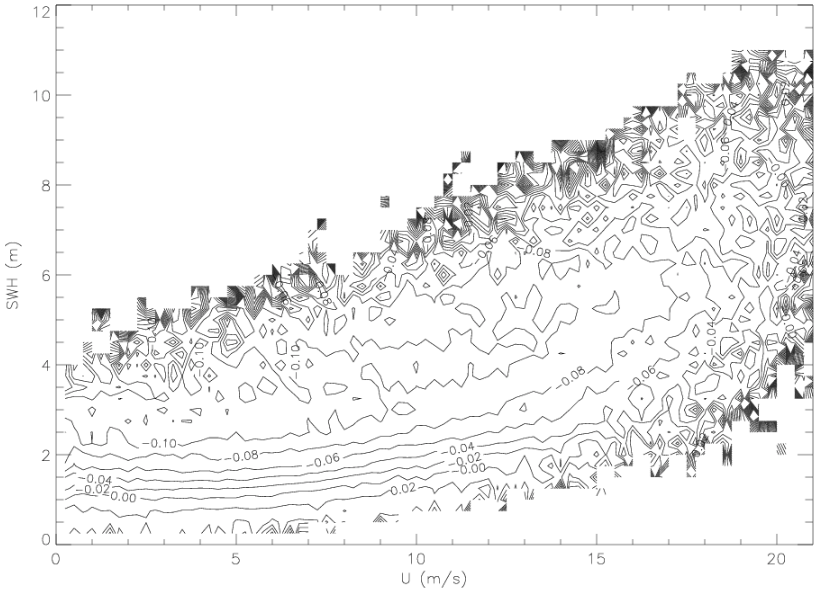

Figure 17 - Height correction, mean of the crossover difference

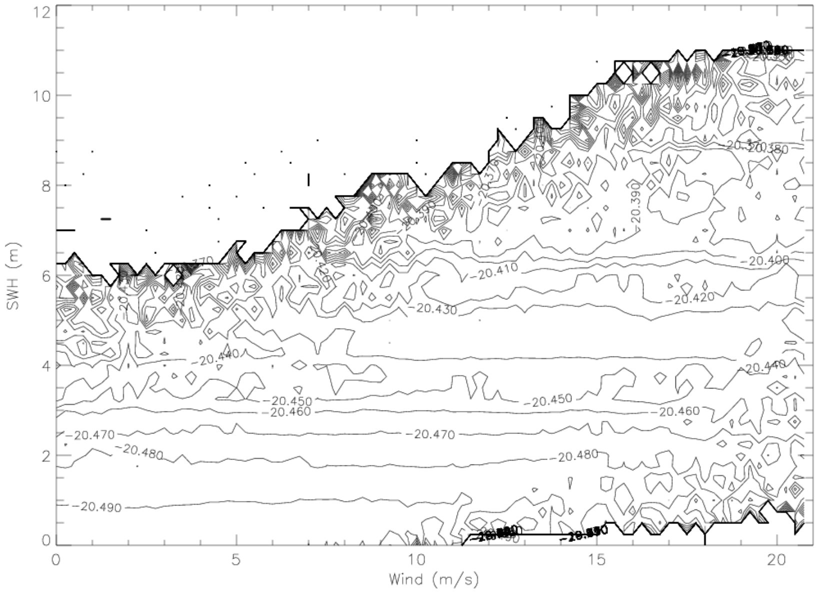

Figure 18 - Mean of the height correction (year 2000)

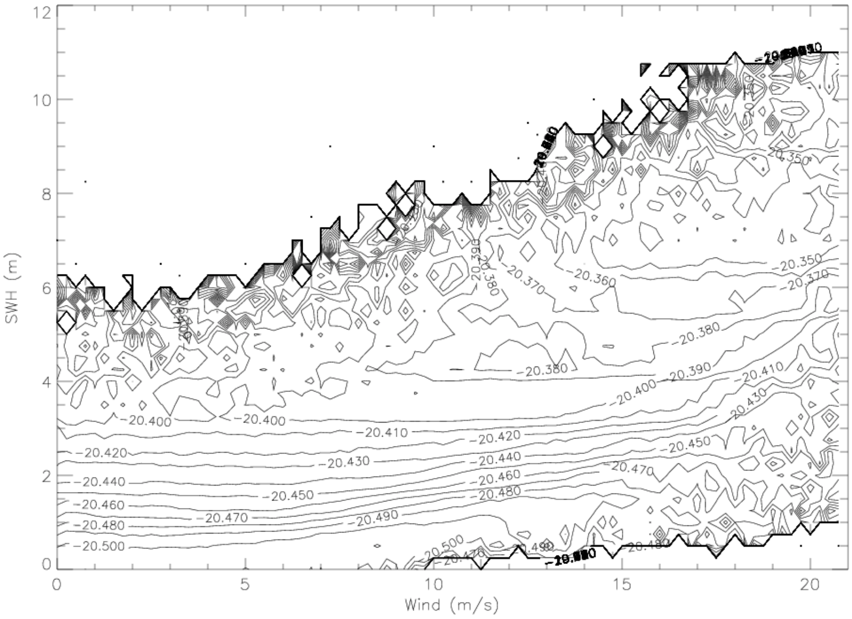

Figure 19 - Height correction, ascending tracks

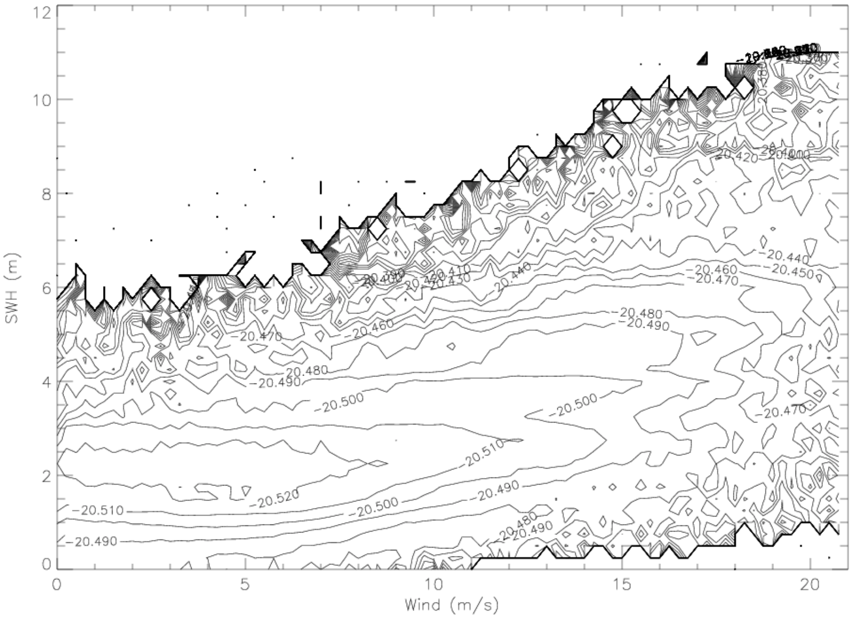

Figure 20 - Height correction, descending tracks

The main contributions to the height correction are the Doppler correction and the SWH and attitude dependant correction. The constant terms cancel out when forming the crossover difference. The Doppler correction is computed from the orbit data (as explained in the section 2.2.3) and the part of the correction depending of SWH and attitude is then recomputed using equation (3). As we know that this correction depends on SWH, it could probably explain the observed variations.

For the along-track data, the Doppler correction has a zero mean since the height rate has a zero mean. Figure 21 and 22 show the Doppler correction for the ascending and descending tracks. As expected, they are of opposite signs. Considering all the along-track data, the Doppler correction is cancelled. Consequently, the height correction mainly reveals the effect of the SWH and attitude correction.

One can notice that the ascending Doppler correction matches the ascending height correction while the descending figures are different. It means that the part of the height correction depending on SWH and attitude is different for ascending and descending tracks.

The same analysis is done at crossovers looking at the Doppler correction via the height rate. Surprisingly, the Doppler correction shown on figure 23 and the height correction (figure 17) have the same magnitude and variations as a function of waves and wind speed but of opposite signs! It means that the Doppler correction is the dominant part in the height correction and above all, it is well correlated with SWH in the part of the domain where the gradient variations have been noticed.

It also means that the crossover differences of the SWH and attitude correction present almost no signature in the (U,SWH) plane. As it is shown on figure 24, it is constant for SWH less than 3m and it cannot explain the gradient dynamics noticed for SWH < 2m. Above 3m, the discontinuities for different values of SWH are dominant in the correction difference. They are probably an effect of the gate index used to compute the correction.

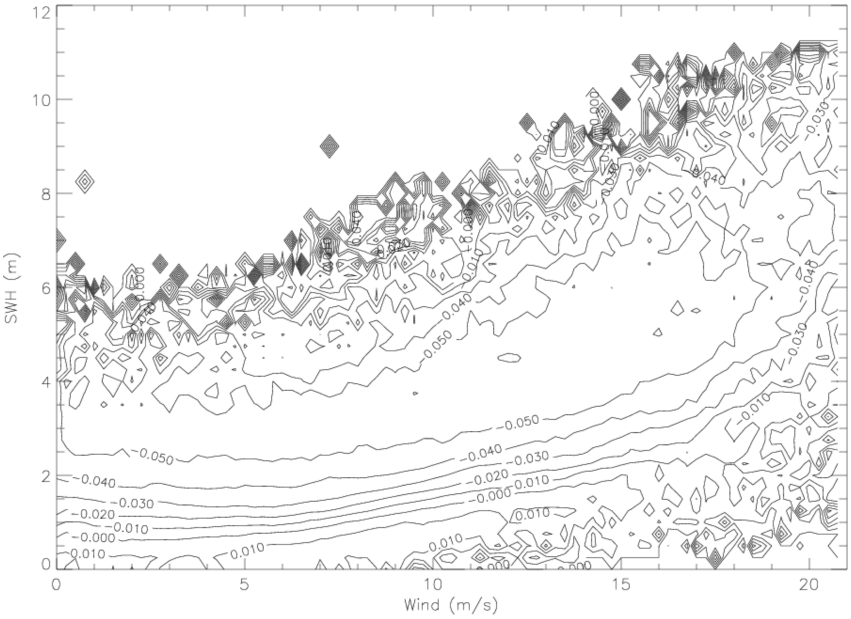

Figure 21 - Doppler correction, ascending tracks

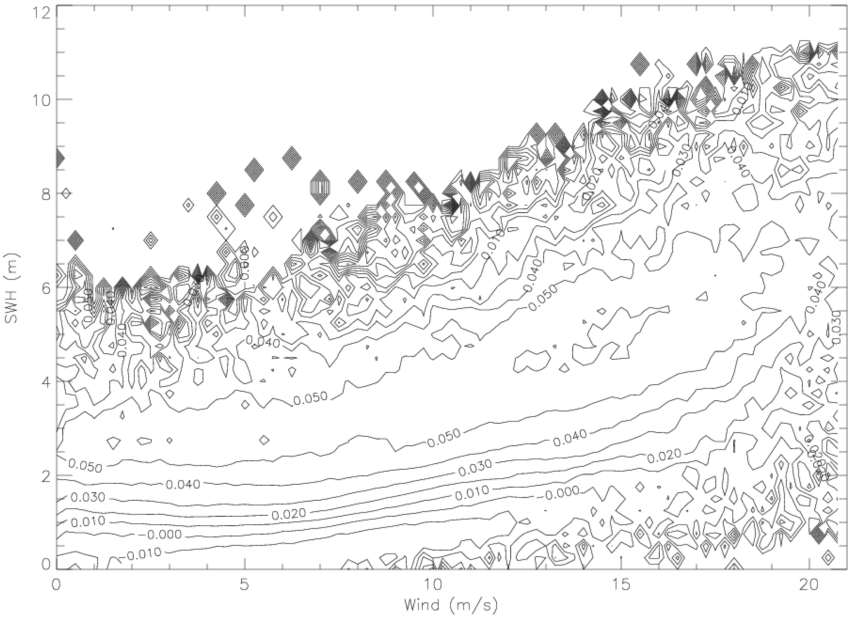

Figure 22 - Doppler correction, descending tracks

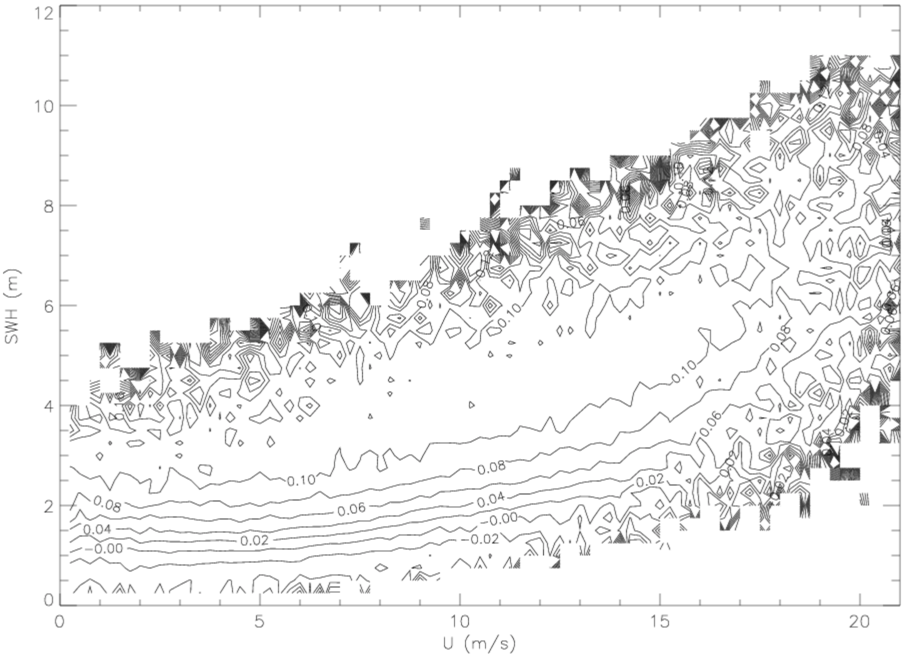

Figure 23 - Doppler correction, mean of the crossover difference

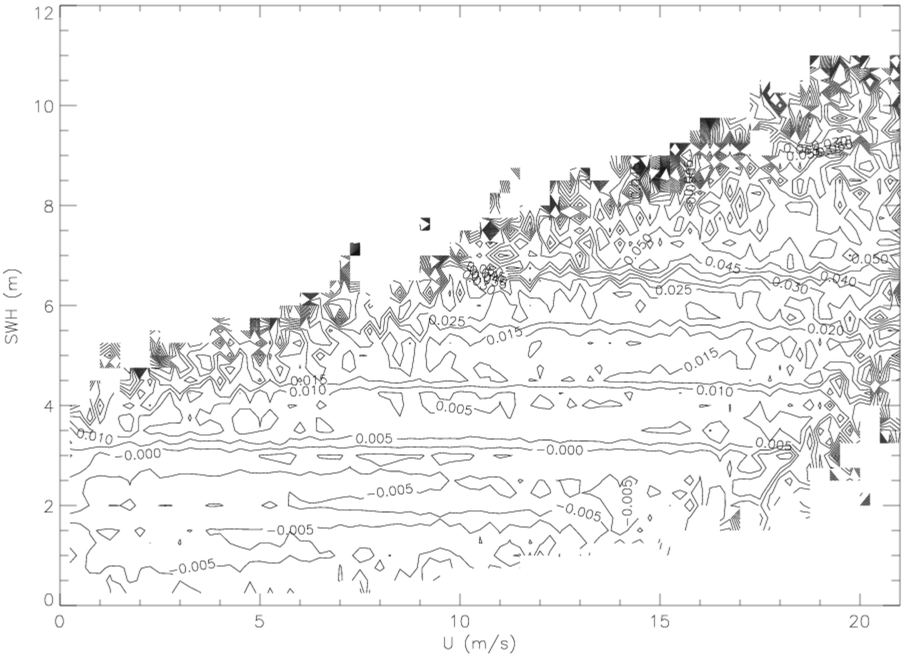

Figure 24 - Height correction(SWH,Att), mean of the crossover difference

To sum up, the Doppler correction has no effect in the along-track data and is emphasized in the crossover differences whereas the SWH and attitude correction is present in the along-track data and it is cancelled in the crossover differences. It indicates that it is more likely the Doppler effect which can explain the SWH gradient appearing in some of the SSB estimates.

Figure 25 shows the evolution of the mean of the crossover differences of the height rate since it is proportional to the Doppler effect. Again, the variations seem to be correlated with the SSB signature and the lower values of 13 m/s match the height correction peaks noticed on figure 16. This analysis suggests to check if there is some time-tag bias in the data, which could affect the SSB estimation performed on the crossovers.

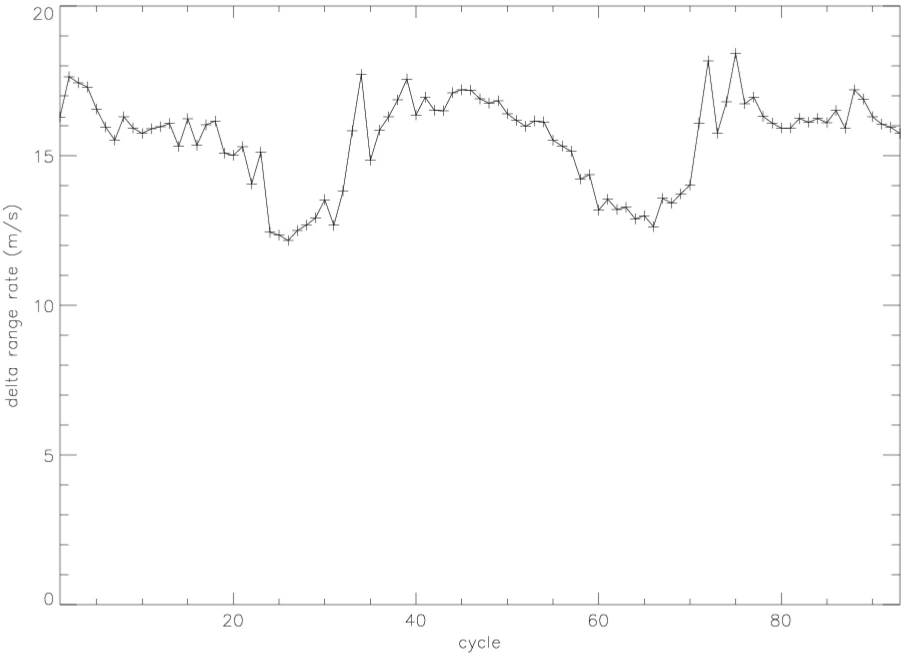

Figure 25 - Mean of crossover difference of the height rate (m/s)

The time tag bias is thus computed for each 10 day data set by fitting the SSH differences (corrected here with the BM1 model given in the product) with differences of height rate. The temporal variations of this bias is given in figure 26. It varies between -1.2 ms and -0.1 ms with an important temporal signature, correlated with the variations observed in the previous figures.

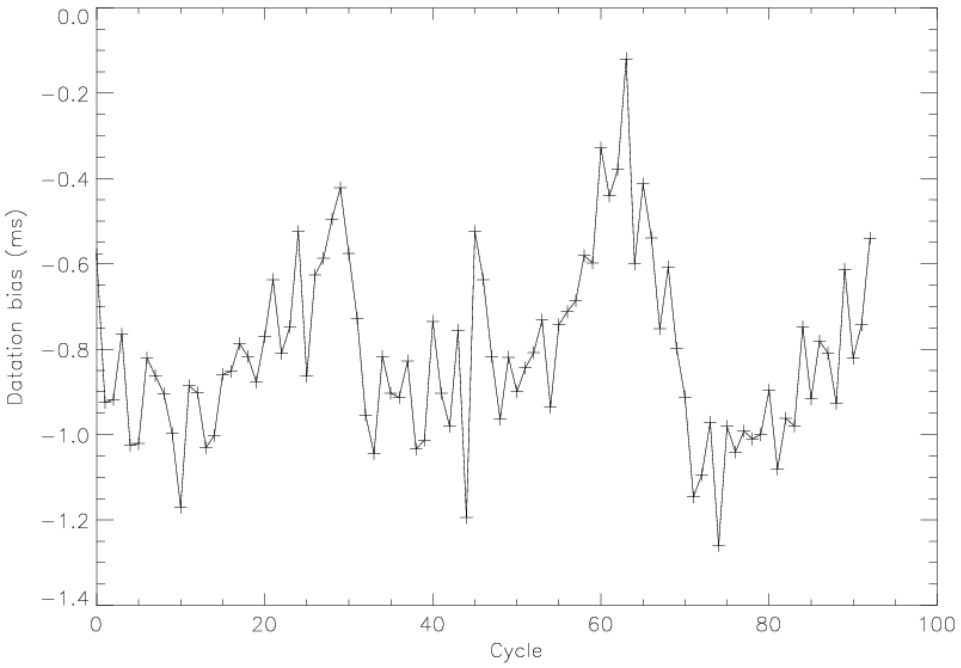

Figure 26 - Mean of crossover time tag bias (ms)

In the next section, we correct the SSH differences for the time tag bias before estimating the SSB.

3.1.3. Effect of the time tag bias on the sea state bias estimation

The SSB estimation is performed in the same conditions on all the 10 days crossover data sets removing the time tag bias before the estimation. Figure 27 presents the result obtained on the first data set which contains 33 estimates. The result is very similar to figure 10 for the general shape of the SSB but the magnitude is more in line with what we expect.

Figure 28 shows the difference between this new estimate and the one without correcting for the time tag bias. In this figure, the SWH gradient appears clearly for SWH<3m. This means that the time tag bias induces a gradient of 4% of SWH on the crossover SSB estimation!

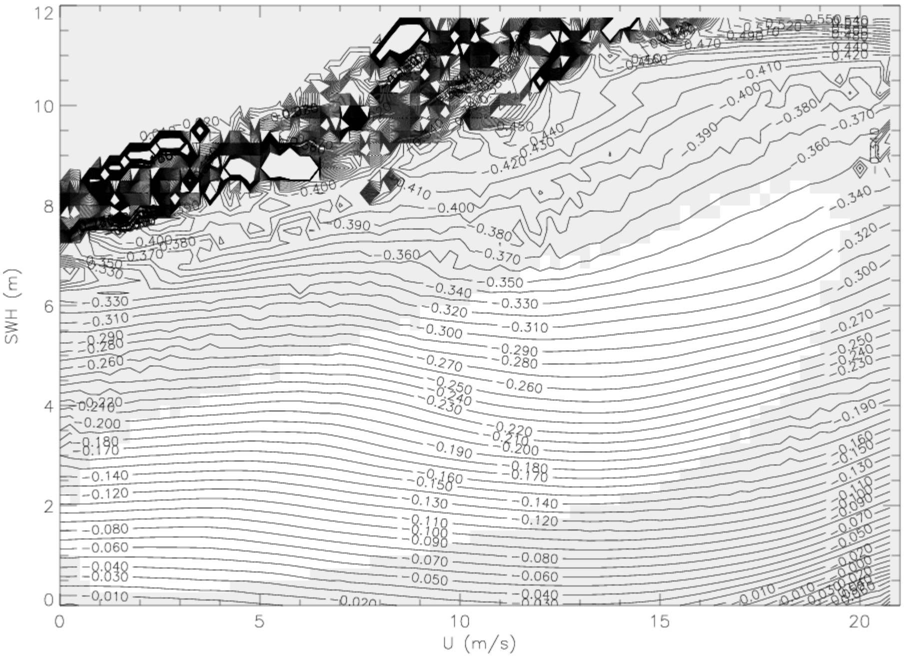

Figure 27 - SSB estimate for the CROSS1 data set, after removing the time tag bias

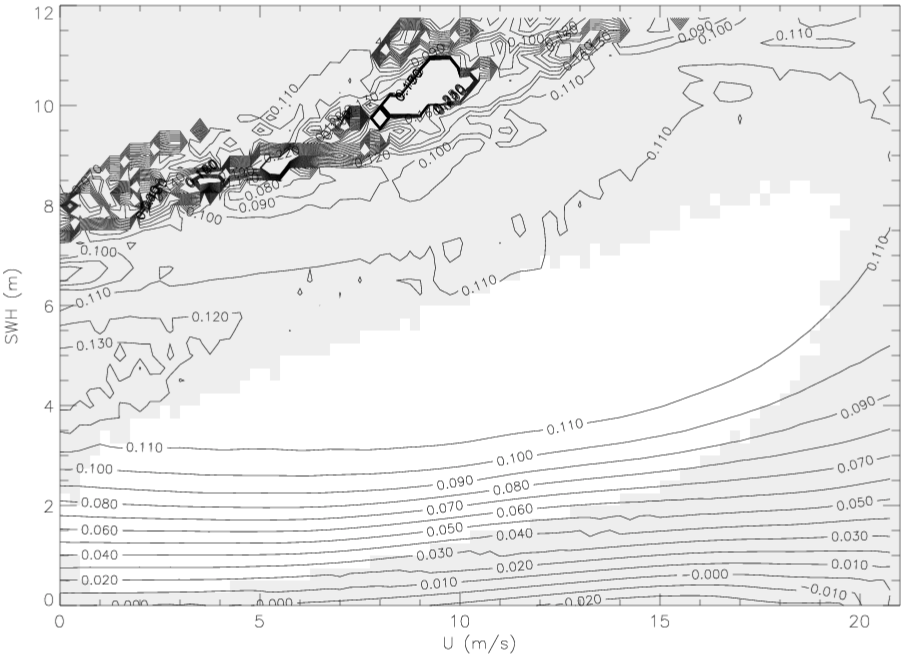

Figure 28 - Difference SSB corrected for the time tag bias - SSB Crossover initial

The next figure presents the SSB estimation using all the 93 crossover estimates after the time tag bias has been removed. In this case, smaller smoothing bandwidths have been used with 0.9m for the waves and 2m/s for the wind speed. One can notice a few ripples close to SWH=4m and U=6m/s which come from the bad quality of some of the individual estimates. It is confirmed by figure 30 which exhibits the estimation variance. It seems that the first part of the estimates are less stable than the second half of the data.

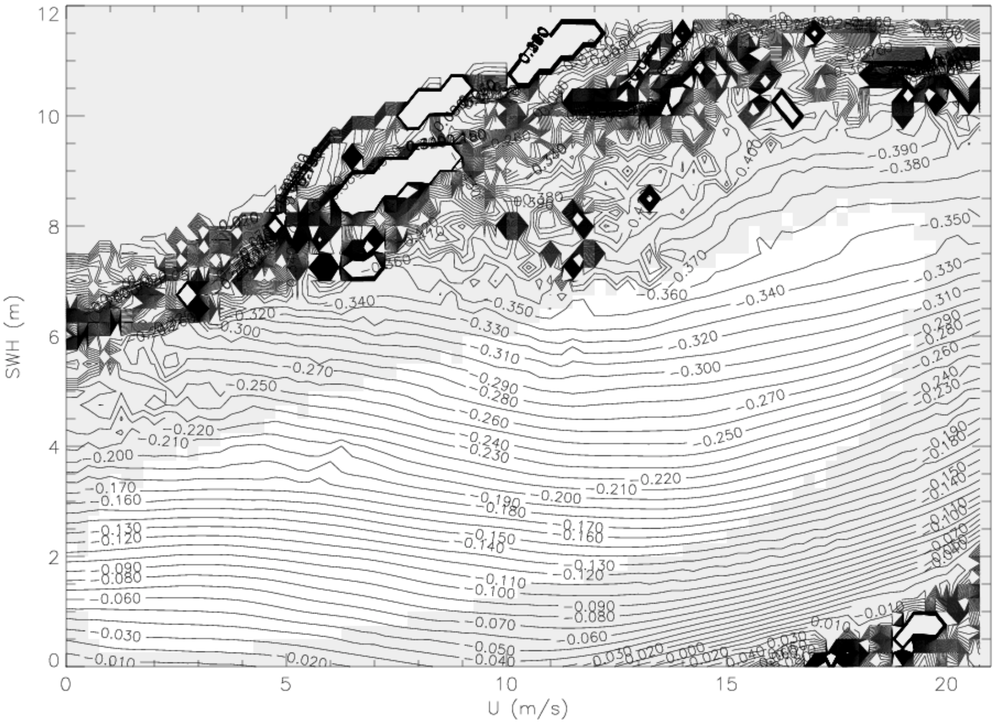

Figure 29 - SSB estimate for the entire data set, after removing the time tag bias (93 data sets)

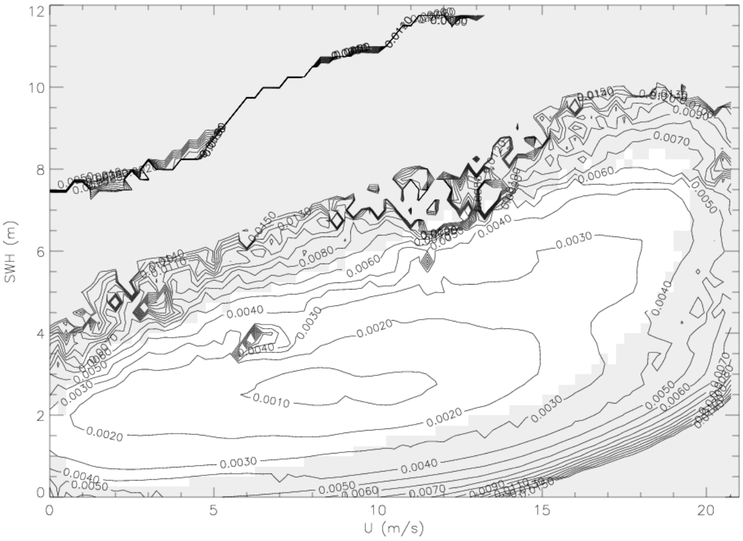

Figure 30 - Estimation variance for the entire data set, after removing the time tag bias (93 data sets)

Figure 31 shows the number of crossover measurements for each 10 day data set. It is clear that the first half of the data sets is less stable because there are too large gaps of data. We decide to select the second half starting with the data set 50 to get an homogeneous data set, with an average of 7000 measurements per data set.

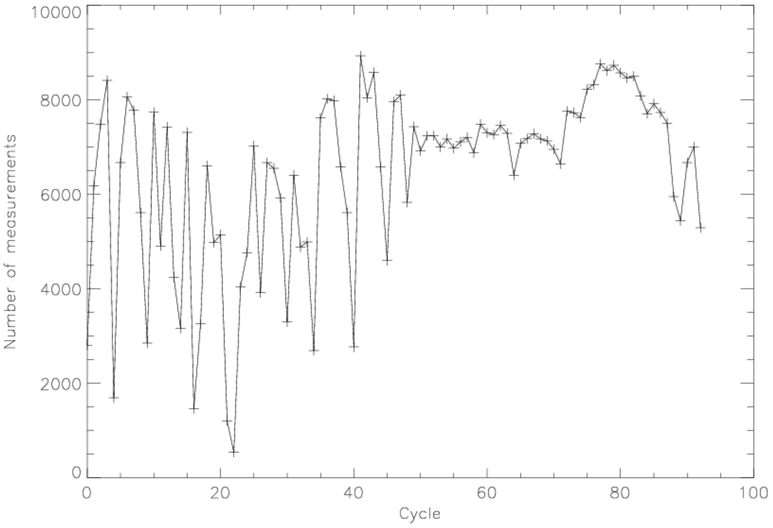

Figure 31 - Number of measurements for the 10 day crossover data sets

The selected SSB estimation at crossovers uses 44 individual estimates, from data set 50 to 93 which spans the period from May 2001 till July 2002, a little bit more than one year of data. The final estimation and the associated variance are given in figures 32 and 33.

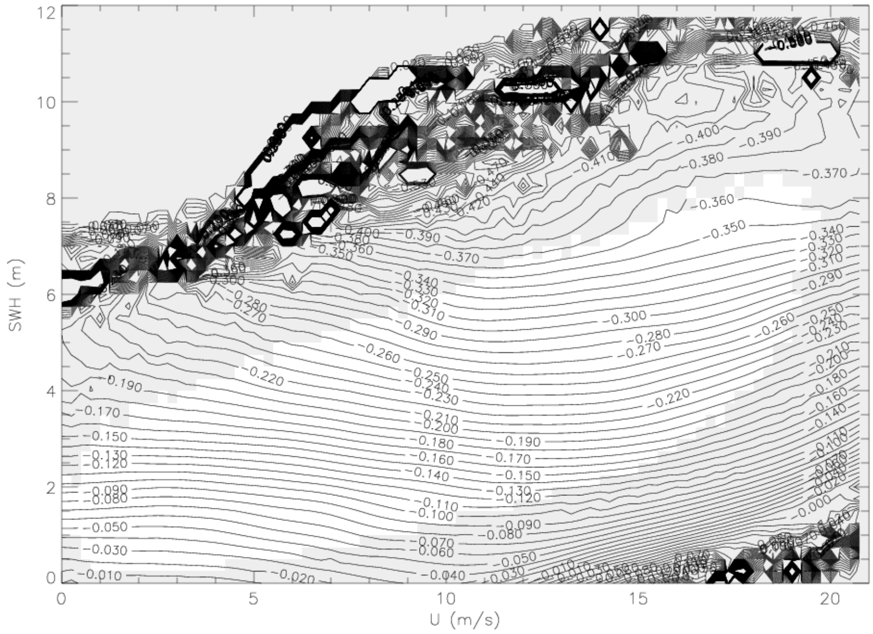

Figure 32 - SSB estimate for the selected data set, after removing the time tag bias (44 data sets)

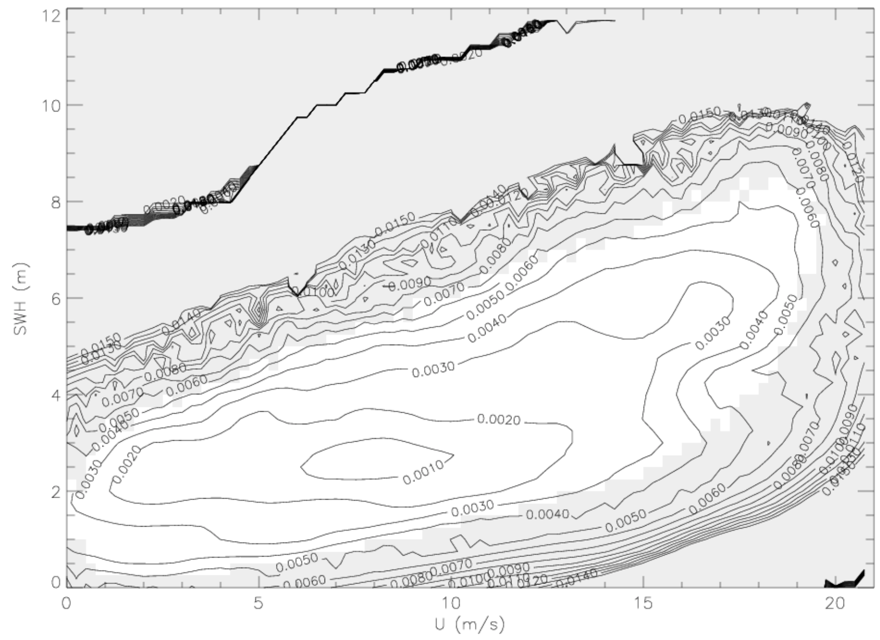

Figure 33 - Estimation variance for the selected data set, after removing the time tag bias (44 data sets)

One interesting point is the analysis of a parametric model BM4 fitted on the same crossover data set, without removing the time tag bias. Figure 34 shows the monitoring of the coefficient related to SWH to check if the BM4 model is able to detect the same trend as the one observed with the non parametric estimates. It is clear that the parametric model does not retrieve the signal observed with the non parametric estimation : the coefficient seems to be centered around -0.04 with variations more likely due to noise. It can be explained by the formulation of the BM4 model which imposes the SSB to be zero at SWH=0m and U=0m/s whereas the non parametric technique lets the retrieved SSB fit the data without imposing any value in this part of the domain where the data become scarce and of poorer quality. This demonstrates the advantage of doing the SSB analysis with the non parametric tools since it can detect and highlight problems where the BM4 model fails to reveal them.

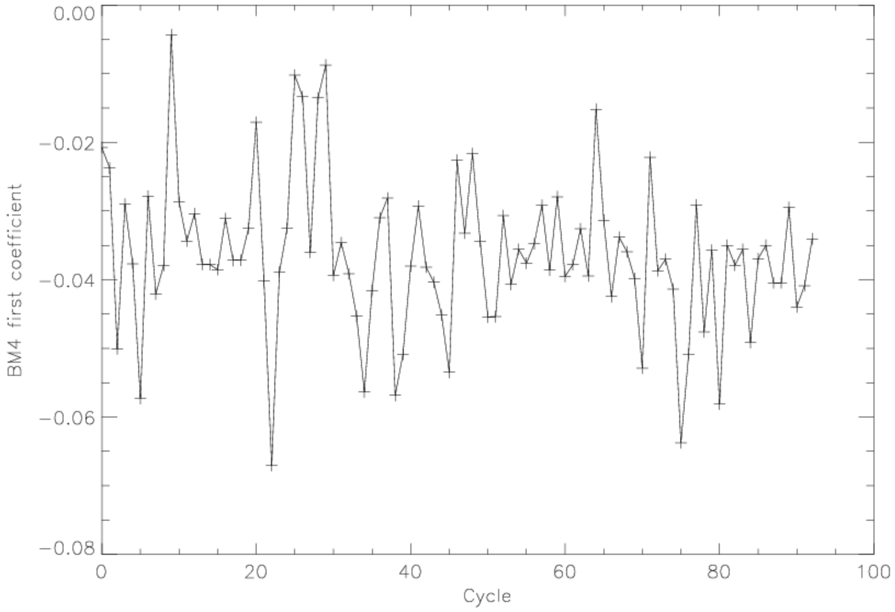

Figure 34 - BM4 coefficient related to SWH

3.1.4. Selection with the latitude

In this section, a simple test is done to evaluate the impact of high latitude data in the SSB estimation at crossover differences. The same data set corrected for the time tag bias is used, removing data with latitudes greater than 60°. It is a way of discarding remaining ice data and, furthermore, it gives less weight to high latitude data in the global distribution of the crossover measurements.

Figure 35 shows the estimation obtained with such a data set over the last 44 cycles and figure 36 the difference between this estimate and the one of figure 32. The difference is a constant for all the data with SWH>2m and one can notice some SWH gradient which appears for the waves less than 2m. It comes from the distribution of very high latitude data which are mainly correlated with low waves. Removing these data modifies the distribution of SSH differences and the SSB derived from it.

These two crossover estimates will be evaluated in section 3.3 with crossover and SLA statistics to check if one of them better explains the data variance.

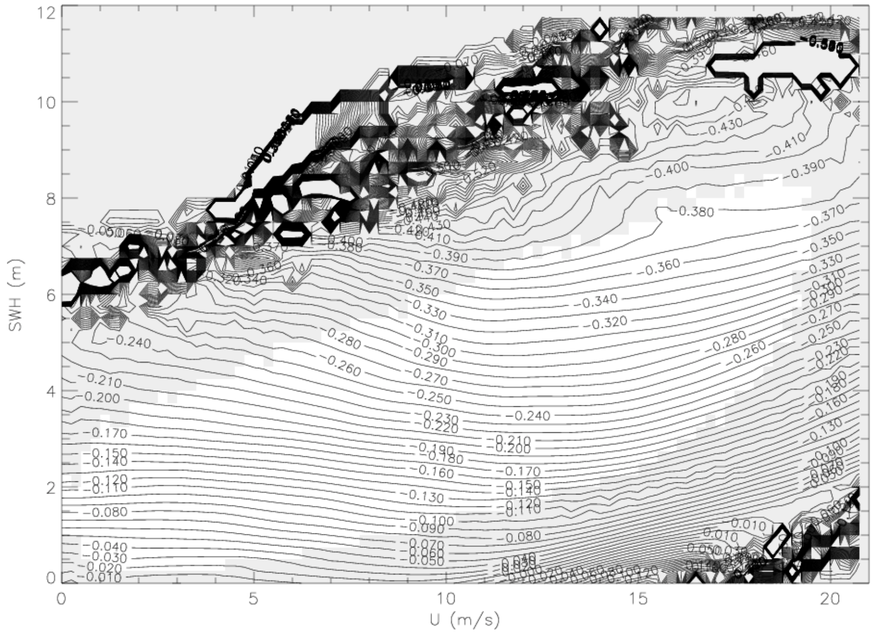

Figure 35 - SSB estimate for the selected data set, after removing the time tag bias and selection |Lat[<60° (44 data sets)

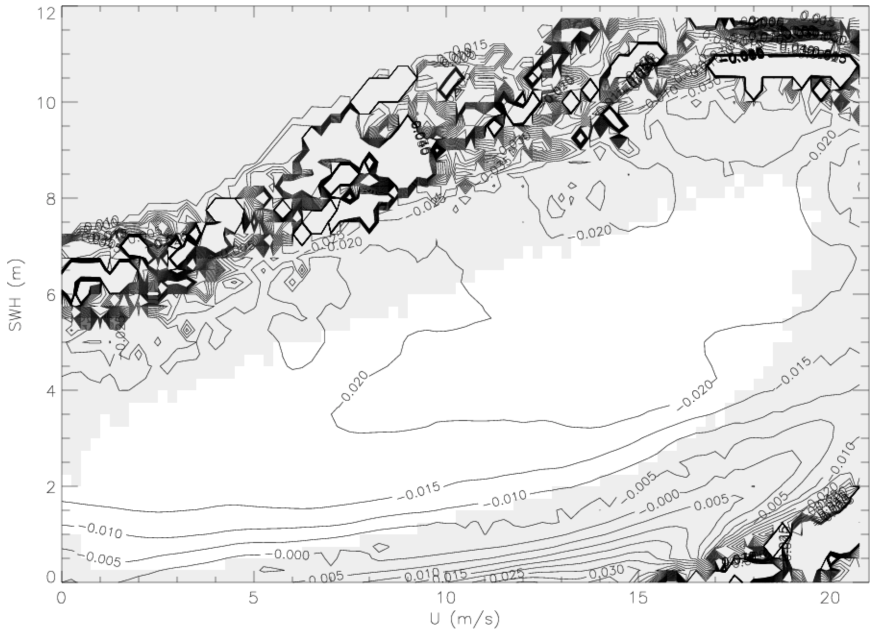

Figure 36 - Difference SSB with |Lat[<60° - SSB corrected with time tag bias

3.2. DIRECT ESTIMATION

In this section, we present the results obtained on the SSB with the direct method, using SLA data on the same period than the one selected for the crossovers ie from May 2001 till July 2002.

Similar corrections are applied to the SSH measurement and the SLA are calculated relative to the CLS 2001 mean sea surface.

The wind speed histogram on each cycle shows a large class of values set to zero. It surely comes from the MCW wind speed algorithm which gives a wind speed set to zero for backscatter coefficients greater than 19.5 dB. All the data with sigma0 greater than 19 dB are discarded which is equivalent to remove wind speed less than 0.25 m/s.

High latitude data are also edited : all the measurements with | lat | > 60° are rejected to discard remaining ice data.

A quick test made with simple average per bin of (U,SWH) has confirmed that the time tag bias has no effect when considering all the direct measurements.

The non parametric technique is used with smoothing parameters which take into account the data density. The computed estimate is then shifted with the initial value obtained for SWH=0m and U=0m/s. For this estimation, it is close to +10cm. Figure 37 shows the estimate finally obtained. The general shape is very close to the crossover estimate. One can notice two small differences. There is a peak for SWH=8m and U>15 m/s which seemed to exist on the crossover estimate but was less marked. The other point is the iso lines which increase in the region of very low winds and high waves. It might come from remaining data of bad quality (rain cells or ice data not edited). This trend is not observed when doing the same analysis on other altimeters like TOPEX, JASON or ENVISAT.

Figure 38 shows the difference between the direct estimate and the crossover estimate of figure 32. We are more interested in the shape of the difference rather than in the magnitude to check if some dependence with SWH and U remains, which would imply that the estimates have retrieved a different structure. There is no marked difference depending on waves or wind speed. For most of the data, the difference is mainly a constant bias around -2cm which comes from the gradient of the direct estimate which is stronger for SWH<0.5m and makes this difference. One can only notice a slight gradient for high winds and low waves.

Figure 39 presents the difference between the direct estimate and the crossover estimate with the selection with the latitude. The shape of the difference is very close to figure 38 for the high waves. The main difference stands for low waves and high winds where there is less organised structure in the difference, which is normal because the latitude criterion removes these measurements.

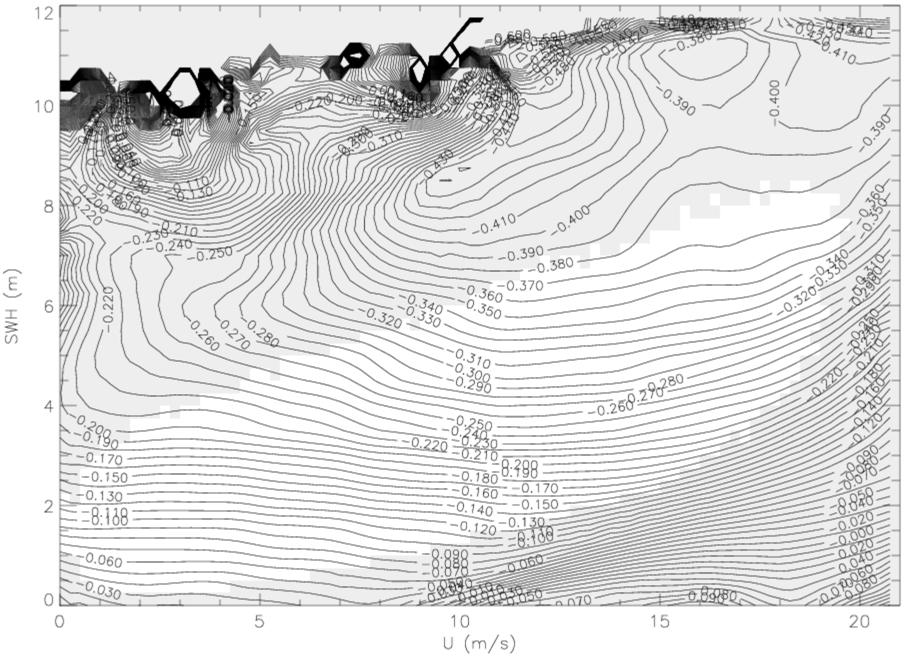

Figure 37 - Direct estimate, May 2001 till July 2002

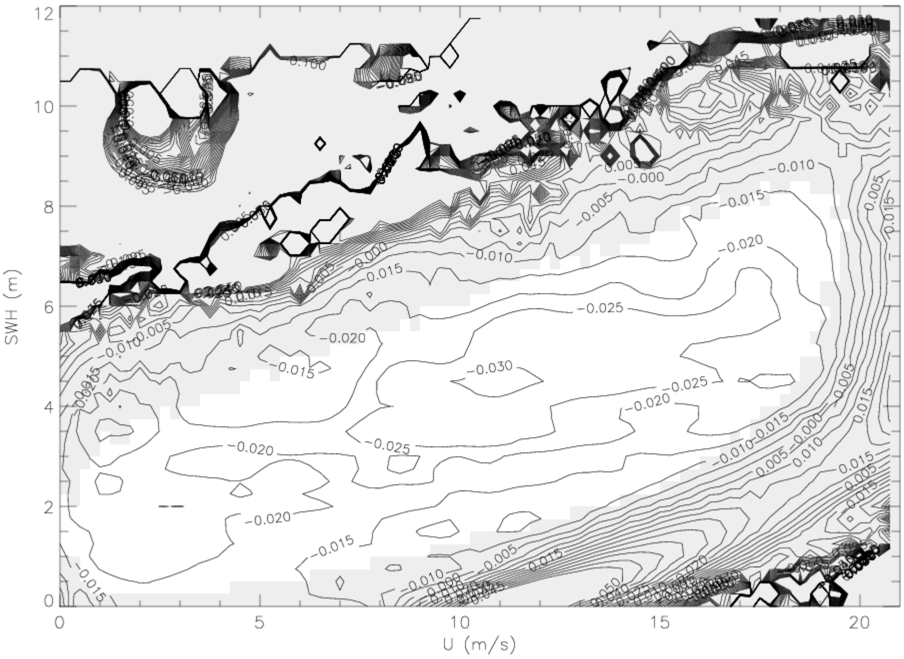

Figure 38 - Difference SSB direct - SSB Crossover corrected with time tag bias

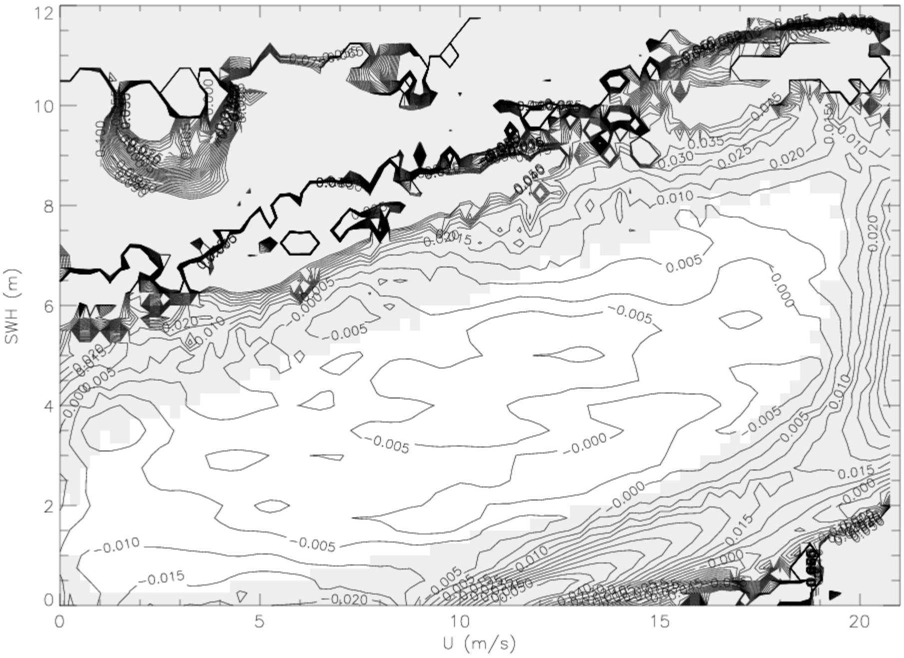

Figure 39 - Difference SSB direct - SSB Crossover corrected with time tag bias and |Lat| < 60°

3.3. RESULTS ON CROSSOVER AND SLA DATA

The three estimates of figures 32, 35 and 37 are now applied to the SSH measurements instead of the BM1 model. The results obtained on crossover and SLA variance are compared in order to find out if one of the estimates better reduces the SSH variance.

For each estimate, the erroneous grid points located on the limits of the data available in the (U,SWH) plane are set to a default value. For very high waves greater than 10m a constant value of the SSB is applied. The SSB value is also imposed to zero for all the grid points with SWH=0m.

The SLA data are selected with a threshold of 50 cm after applying the SSB correction. The crossover data sets are simply the ones used for the SSB estimation after applying the SSB correction.

The three SSB models are compared in terms of crossover variance reduction : the estimation from all crossovers, the estimation from crossovers at latitudes lower than 60° and the direct one. The results are presented relative to the first model (all crossovers) on figure 40.

The crossover SSB estimate explains more variance than the two other estimates, with 0.5 cm^2 in average.

Figure 41 shows the same comparison done on SLA data. The crossover and the direct estimates are very close for almost all the cycles, except a few ones where the direct estimate explains more variance of about 1 cm^2. The first part of the data set (year 2000, till cycle 57) presents more variations in the gain of variance.

The comparison of the two crossover estimates is very noisy, giving no real conclusion on the quality of both estimates.

According to figure 40, the crossover estimate should be selected, since it gives better results on crossover variance. Figure 41 exhibits little difference between the direct and the crossover estimate for most of the cycles. Looking at these results, it seems that the crossover estimate should provide satisfactory results for the SLA analysis and better ones for the crossover analysis.

Figure 42 shows the SLA variance reduction as a function of SWH to check if one of the estimates better explains the variance for some values of SWH. The crossover estimate provides better results than the direct one especially for waves lower than 6m, with a difference in the explained variance of about 1 cm^2 between the two methods. The waves between 9m and 10m differ from the other classes of SWH but there are only a few points in these ranges.

Comparing the two crossover estimates, it seems that the crossover without any selection on the latitude behaves better, especially for the waves between 2m and 6m.

In the light of all these results, we can conclude that the crossover estimate of figure 32 should be selected for GFO sea state bias.

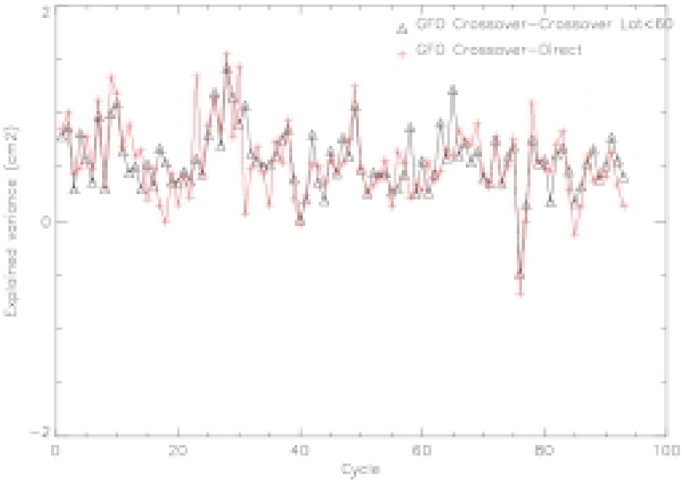

Figure 40 - Crossover explained variance between 3 SSB models (10 day data sets)

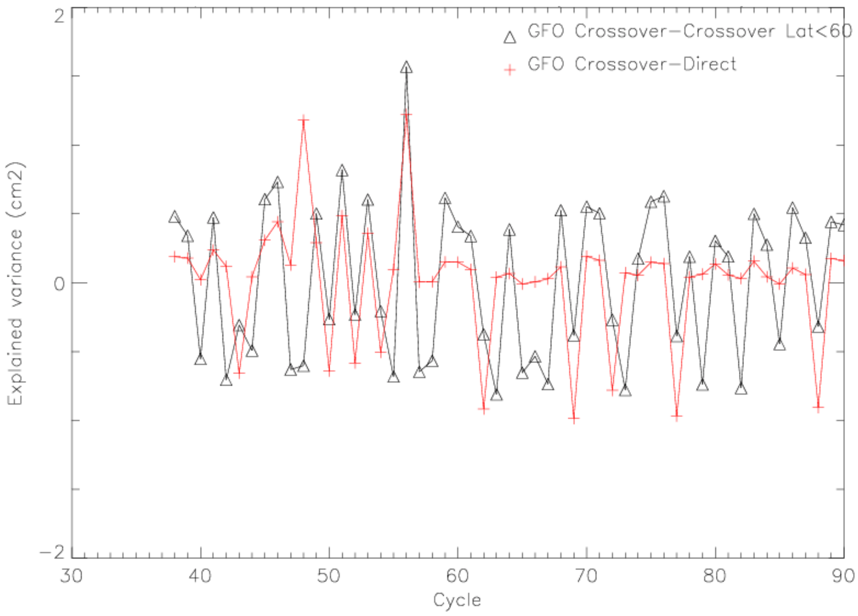

Figure 41 - Explained variance between 3 different SSB models on SLA data, for GFO 17 days cycles

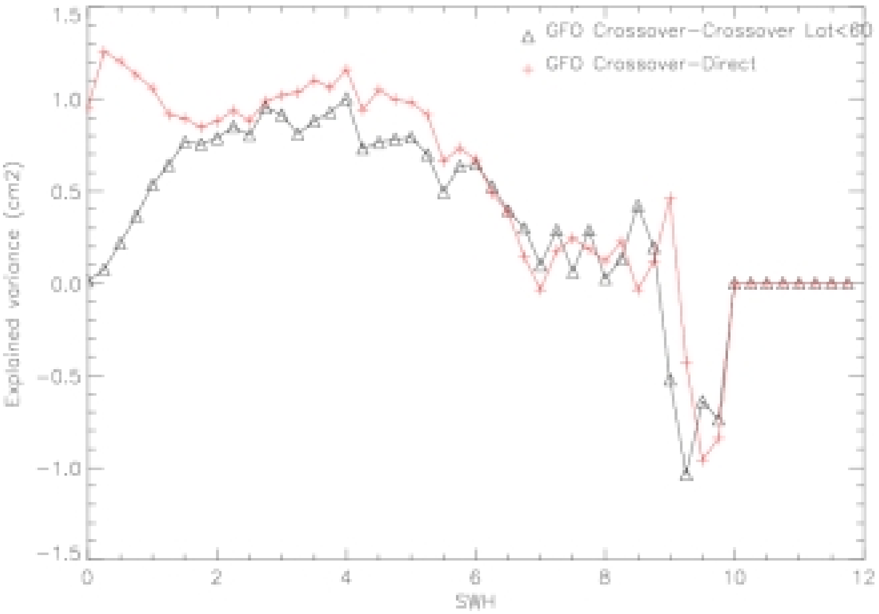

Figure 42 - Explained variance per SWH class between 3 different SSB models on SLA data

3.4. FINAL SSB ESTIMATE

Figure 43 shows the relative SSB (SSB/SWH) for the crossover estimate selected in the previous section. The magnitude varies between -4.4% for the highest waves and -7% for the underdeveloped seas. This order of magnitude is greater than the one obtained for TOPEX but it is more in agreement with JASON 1 and ENVISAT. One can notice the relative SSB increases for wind speeds less than 12m/s and decreases for higher values.

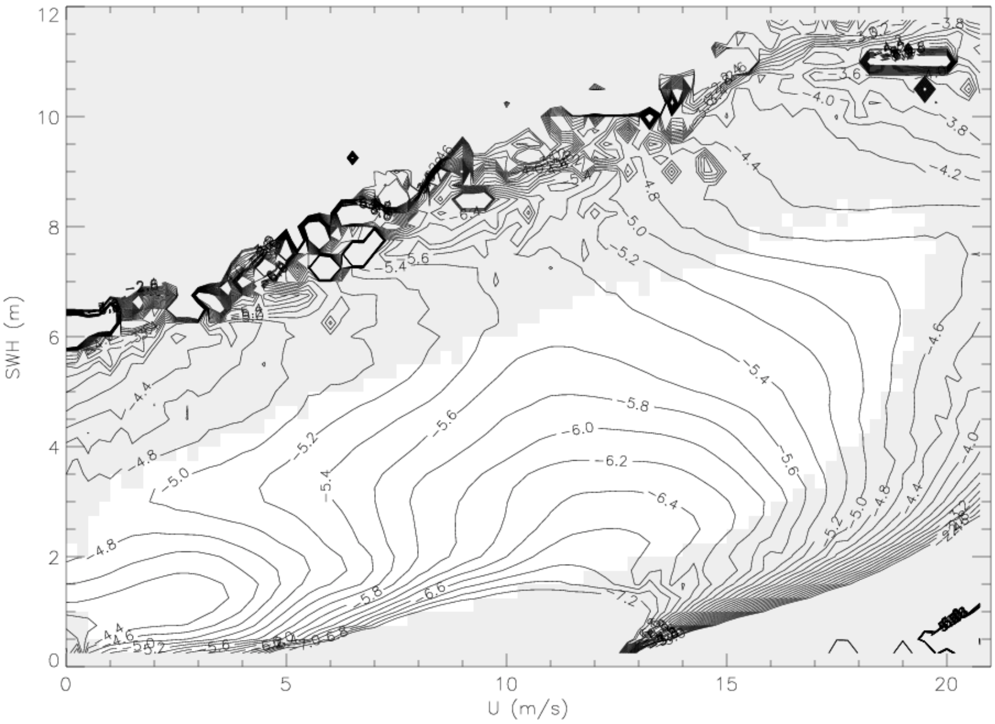

Figure 43 - Relative SSB, Crossover estimate corrected with time tag bias

Figure 44 exhibits the difference of SSB between the parametric BM1 model from the product and the crossover estimate finally selected. The shape clearly shows the influence of the wind speed with the change of trend at U=12m/s : the difference increases for U<12 m/s and then decreases for higher winds. The difference is smaller for low waves and low winds where the BM1 model is not so bad since, in these regions, the SSB is mainly linear with SWH. The difference can be as large as 6 cm, which is not negligible. Thus, correcting with this new SSB should largely improve the data quality.

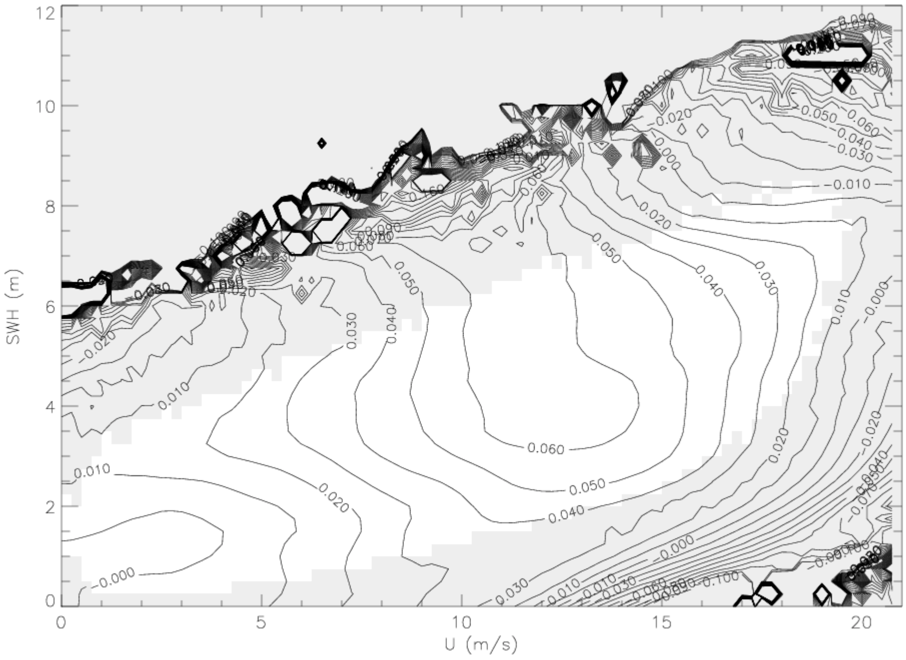

Figure 44 - Difference BM1 model (-0.045*SWH) - SSB Crossover corrected with time tag bias

Figure 45 shows the crossover variance reduction, using the non parametric SSB estimate instead of the BM1 model of the products. For 17 day crossovers, the new SSB model reduces the variance between 2 cm^2 and 4 cm^2 for almost all the cycles. In this analysis, the time tag bias was not corrected.

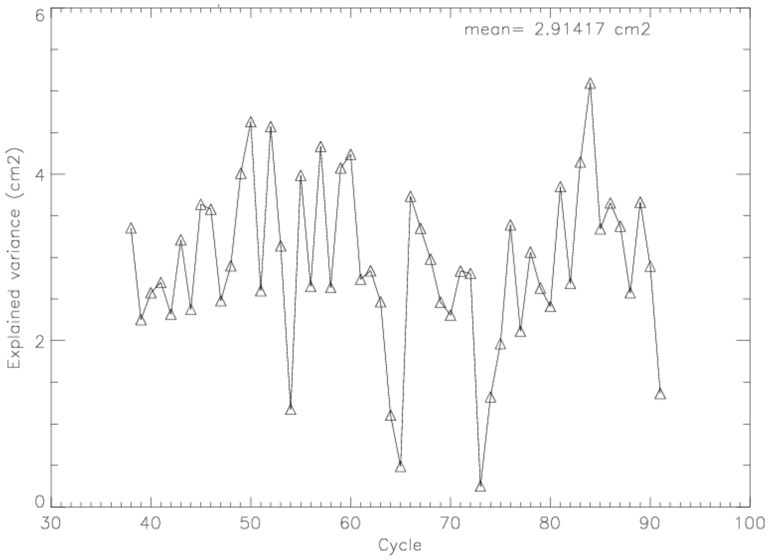

Figure 45 - Crossover explained variance between BM1 model (product) and NP estimate, 17 day crossover

CONCLUSION

The GFO GDR products have been processed from cycle 73 to cycle 91 which spans 2.5 years of data from January 2000 till July 2002.

The data revealed no critical issue dealing with the geophysical corrections. For the altimeters parameters (height, SWH and sigma0), no particular trend has been detected, except for the quantification of SWH which has no real impact on the non parametric estimation processing. A lot of tracks have also been removed indicating large orbit errors but some dubious data still remain. One worrying point is the waveform attitude which is not stable in time. The data editing has to be improved in order to discard properly ice data and also remove orbit errors.

Particular attention was paid to the attitude algorithm processing and to the part of the height correction derived from it. It shows that the waveform attitude (or the average VATT) varies with time and exhibits a north/south and ascending/descending signature.

Once the data have been validated, estimating the SSB with crossover data was not straightforward since it raised other undetected problems in the data themselves. Therefore, a lot of work has been done on the analysis of the crossover SSH differences to understand the effect on the SSB estimation. It made appear that some time tag bias was present in the GFO data and that this bias varied with time, inducing a very strong SWH gradient on several individual SSB estimates. After correcting for it, the SSB shape and magnitude was more in agreement with what we expected.

Finally, we came out with two consistent SSB estimates derived through crossover and direct methods. The selected SSB presents smooth variations close to the ones observed for the other altimeters. The discontinuities due to the gate index are not revealed as clearly as for TOPEX. The magnitude varies between -4.4% for the highest waves and -7% for the underdeveloped seas. This order of magnitude is greater than the one obtained for TOPEX SSB but it is more in agreement with JASON 1 and ENVISAT.

The direct method has shown an unexpected trend for low winds and high waves. The associated measurements to these sea states have to be characterized in details to determine if a more adapted editing could be applied.

All the results presented in this report provide a first non parametric SSB model for GFO sea state bias, using the products data. This new SSB model reduces the crossover variance of about 2.9 cm^2 on the processed cycles, compared to the actual model given in the products.

It is important to further work on the data to better understand the impact of the height correction depending of SWH and attitude. This correction should be investigated more in details using SDR products to check the wind and waves related variations considering either crossover differences or 1Hz measurements. To improve our knowledge of the sea state bias, it would also be interesting to make an estimation removing this correction to separate the effects between the SSB and such a correction.

Looking at the data after cycle 91 would also be interesting since the attitude has been biased of 0.1 degree during cycle 82 and thus, the height correction should have a different magnitude.

The time tag correction has been calculated over 10 day crossover data sets. It should be done over the GFO 17 day cycle to check the consistency between the two data sets.

The effect of this correction on the SSB is a more tricky thing to understand since it affects the crossover height difference and it is always difficult to understand its impact on the SSB itself through the crossover estimation process.

This study provides an empirical SSB model derived from GFO data which can be used to improve the accuracy of the sea state bias correction. Nevertheless, the stability of such a correction should be monitored with new SSB estimations performed on different cycles. Independently, a continuous monitoring of GFO data should be done to check data quality, as it is done for TOPEX, JASON 1 and ENVISAT.

ANNEXE A RAPPORT DES RESULTATS DE LA CHAINE CALVAL